

# Supplementary Material

Design, synthesis, and biological evaluation of novel FAK scaffold inhibitors targeting the FAK-VEGFR3 protein-protein interaction.

Priyanka N. Gogate <sup>a, ‡</sup>, Manivannan Ethirajan <sup>a, ‡</sup>, Elena V. Kurenova <sup>b, d, \*</sup>, Andrew T. Magis <sup>c</sup>, Ravindra K. Pandey <sup>a, \*</sup>, and William G. Cance <sup>b, d, \*</sup>

<sup>a</sup>Department of Cell Stress Biology/ PDT Center Roswell Park Cancer Institute, Buffalo, NY 14263, U.S.A

<sup>b</sup>Department of Surgical Oncology, Roswell Park Cancer Institute, Buffalo, NY 14263, U.S.A

<sup>c</sup>Center for Biophysics and Computational Biology, University of Illinois at Urbana-Champaign, Urbana, IL 61801, U.S.A

<sup>d</sup>CureFAKtor Pharmaceuticals, Orchard Park, NY 14127, U.S.A

\*corresponding authors

## Contents

Fig. S1-S20: Copies of <sup>1</sup>H and <sup>13</sup>C NMR spectra of compounds

Table S1: Table containing Log P of all compounds

Fig. S21: Molecular docking of analog **27**

Fig. S22: Molecular docking of analog **28**

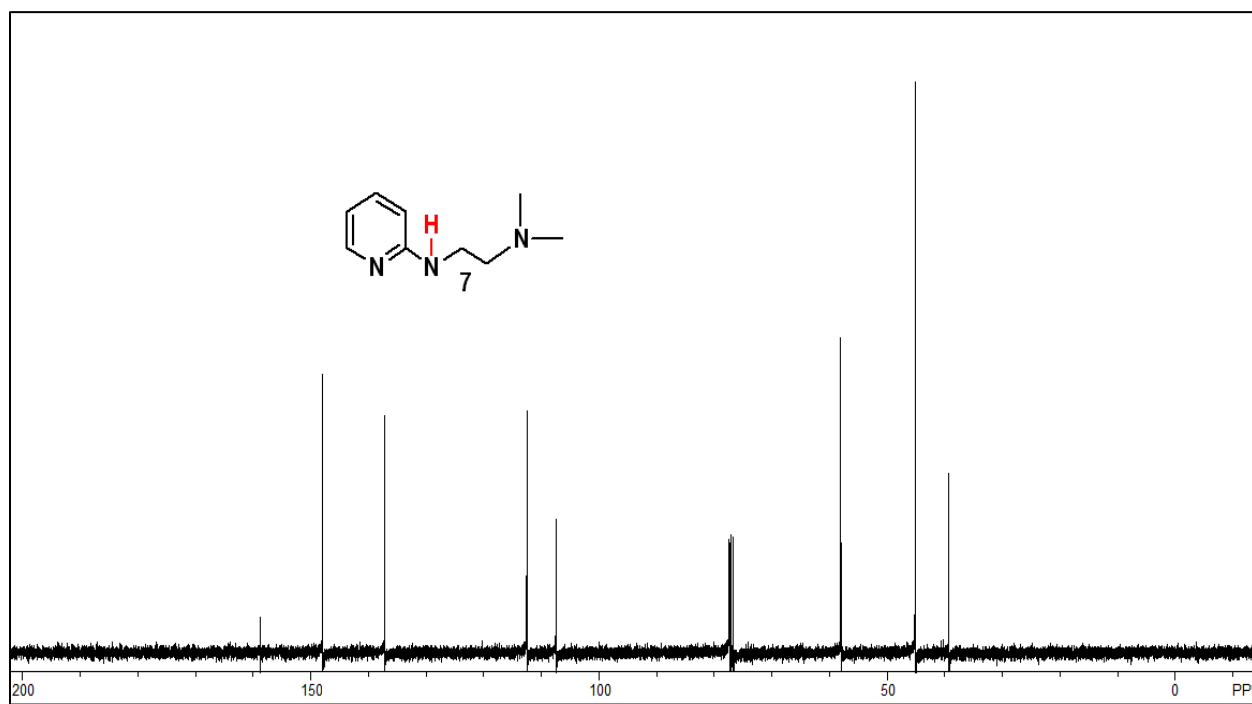
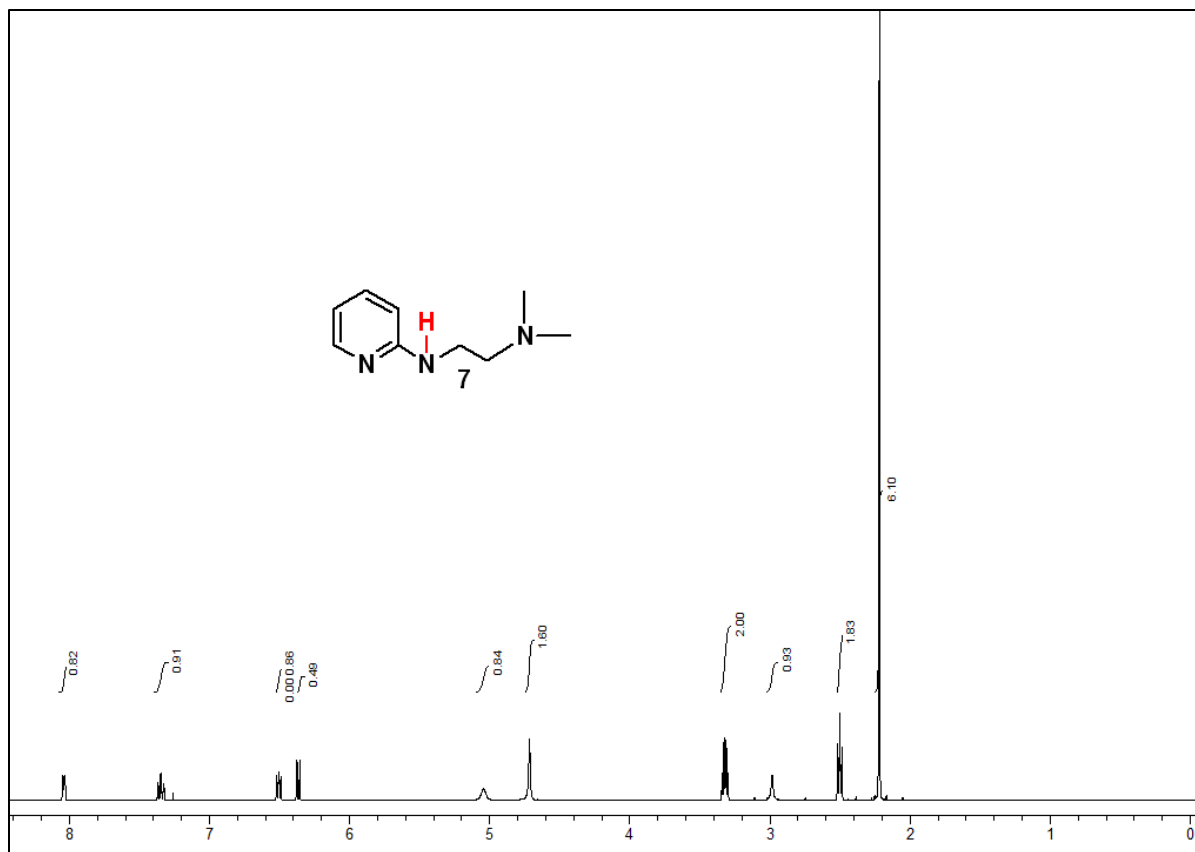


Figure S1

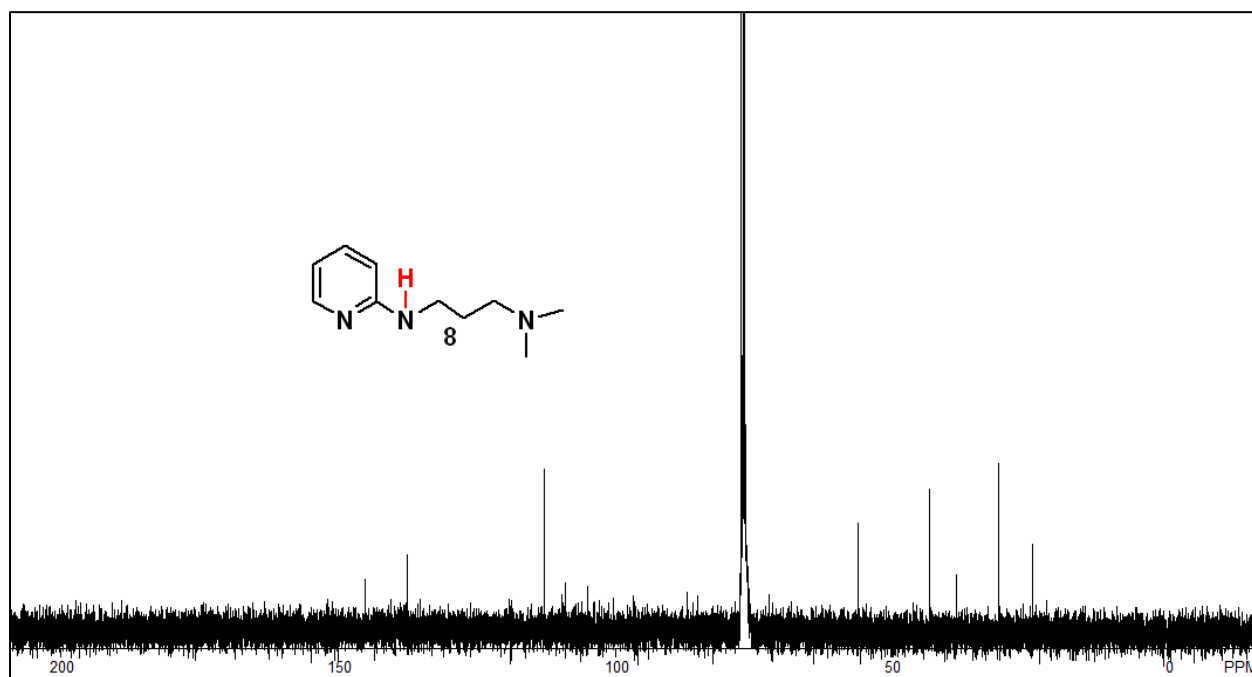
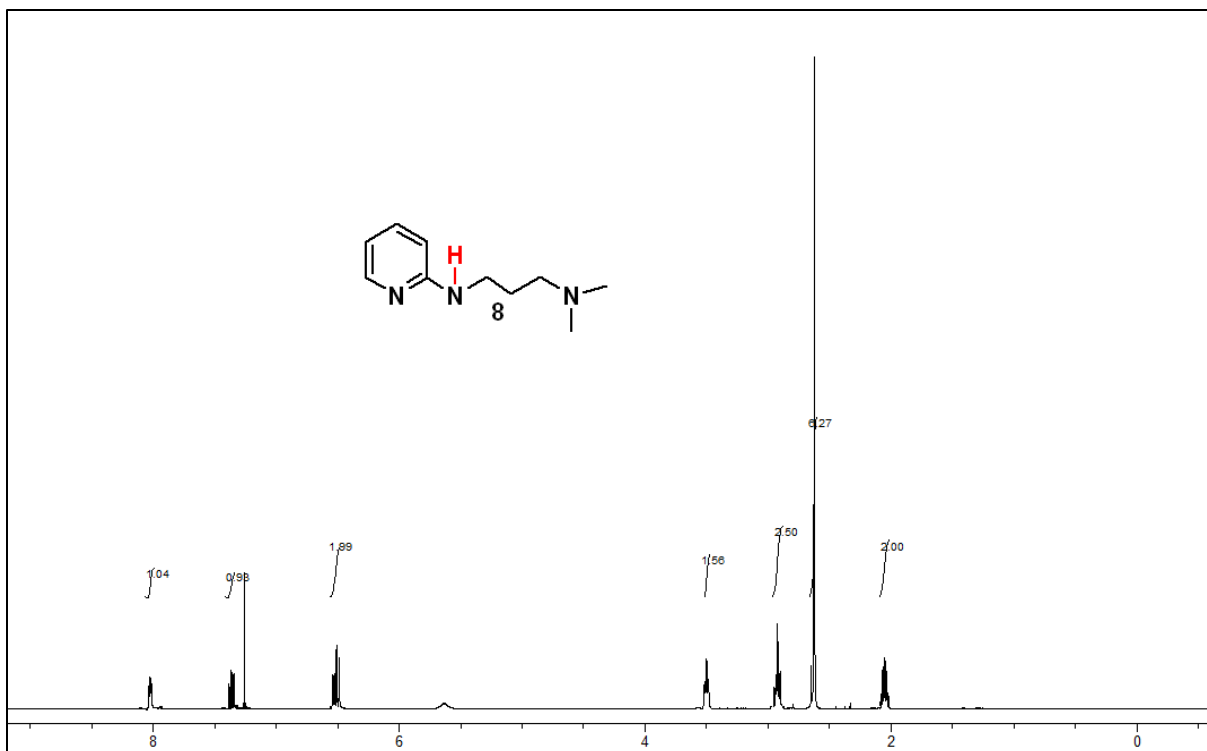


Figure S2

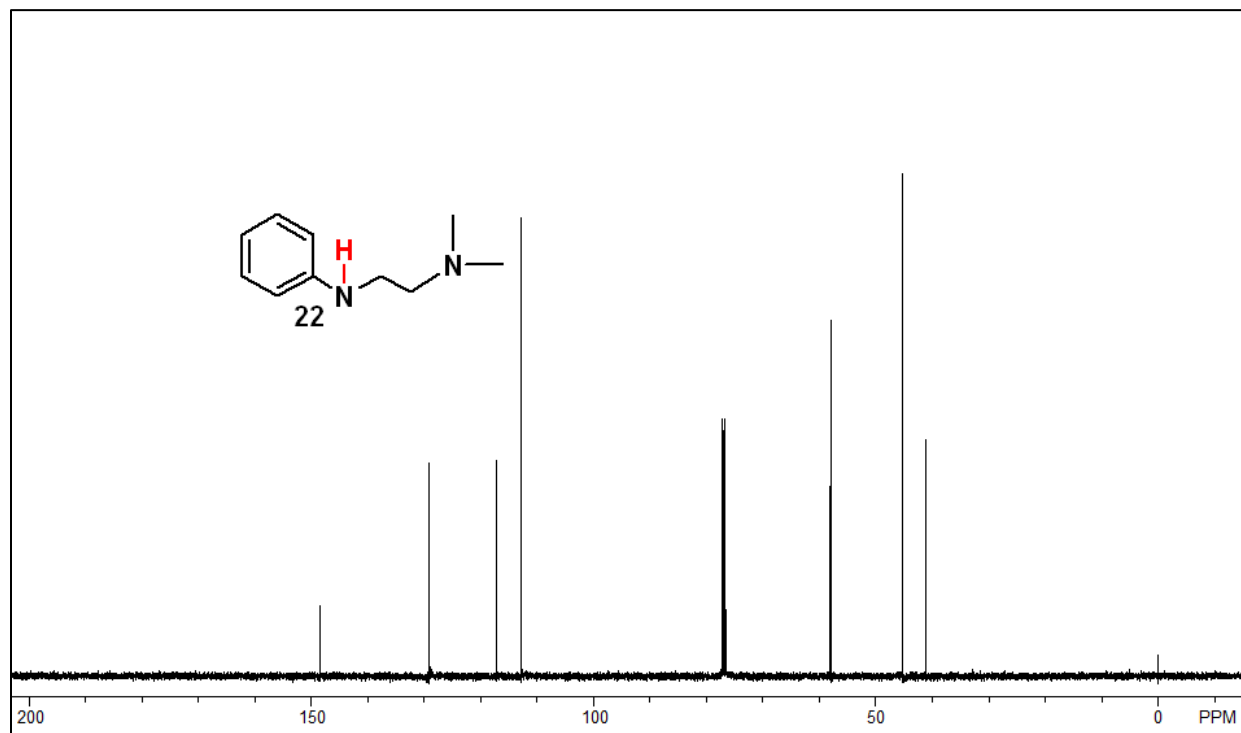
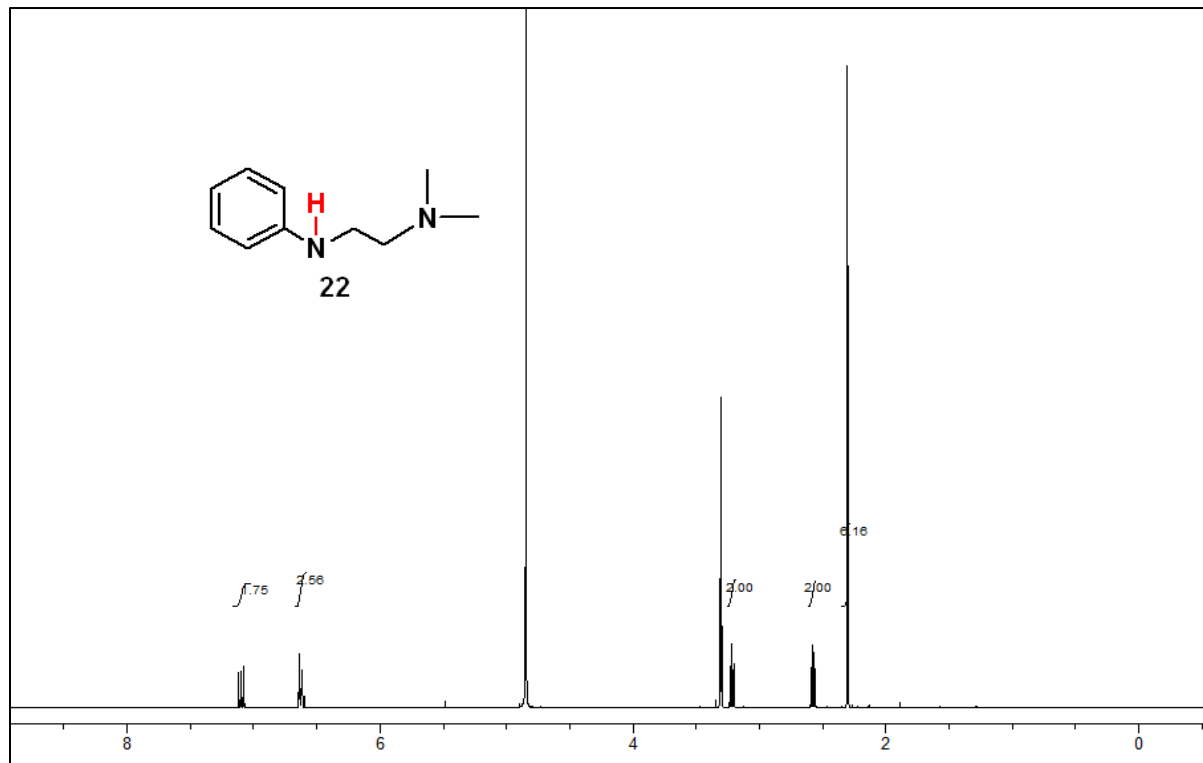


Figure S3

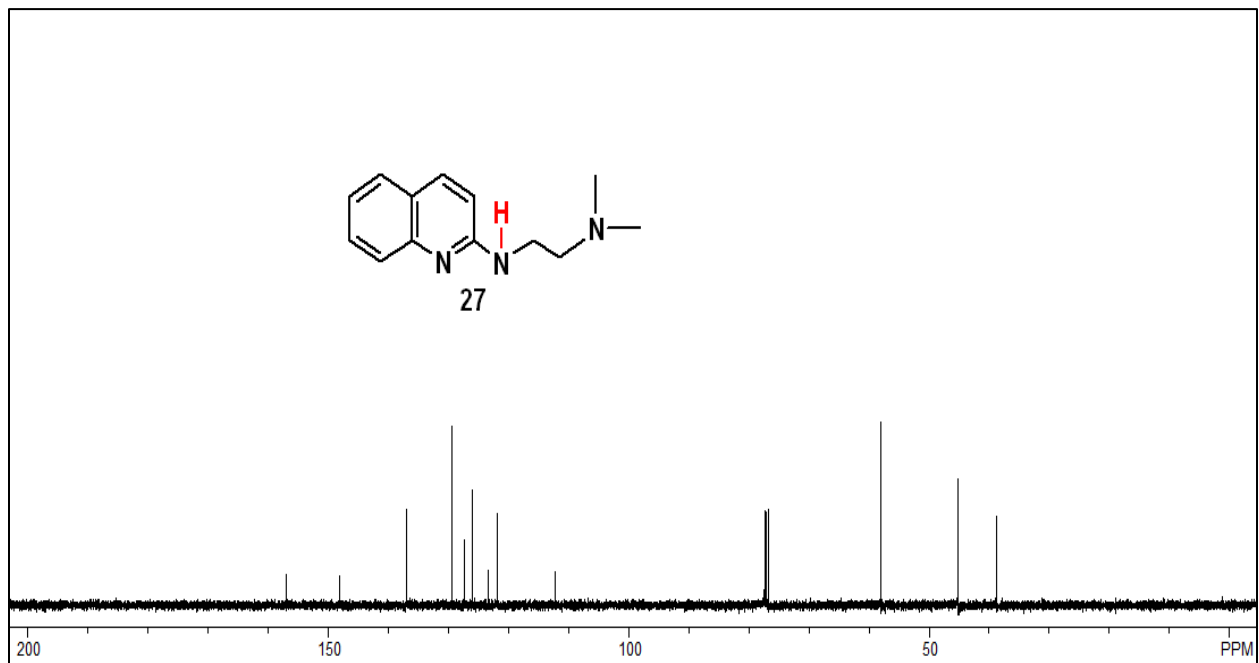
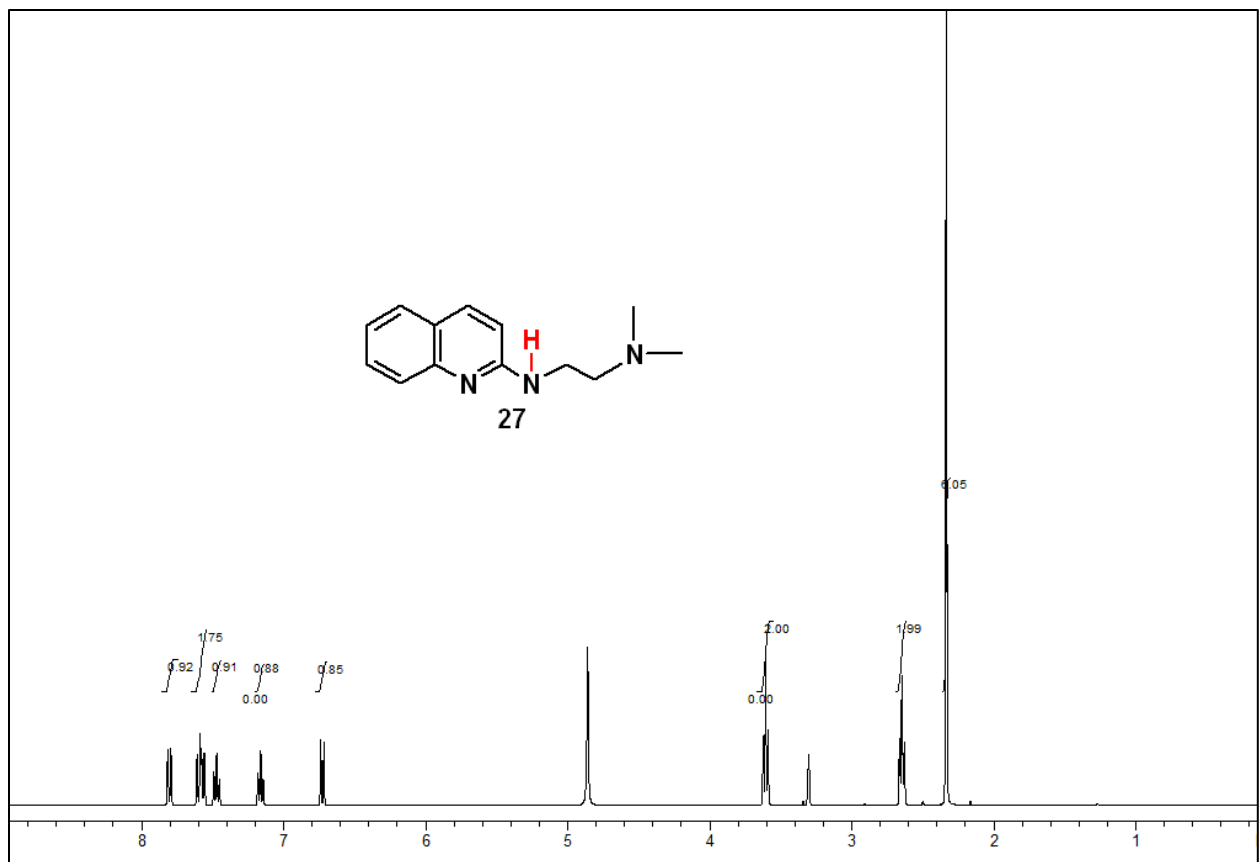


Figure S4

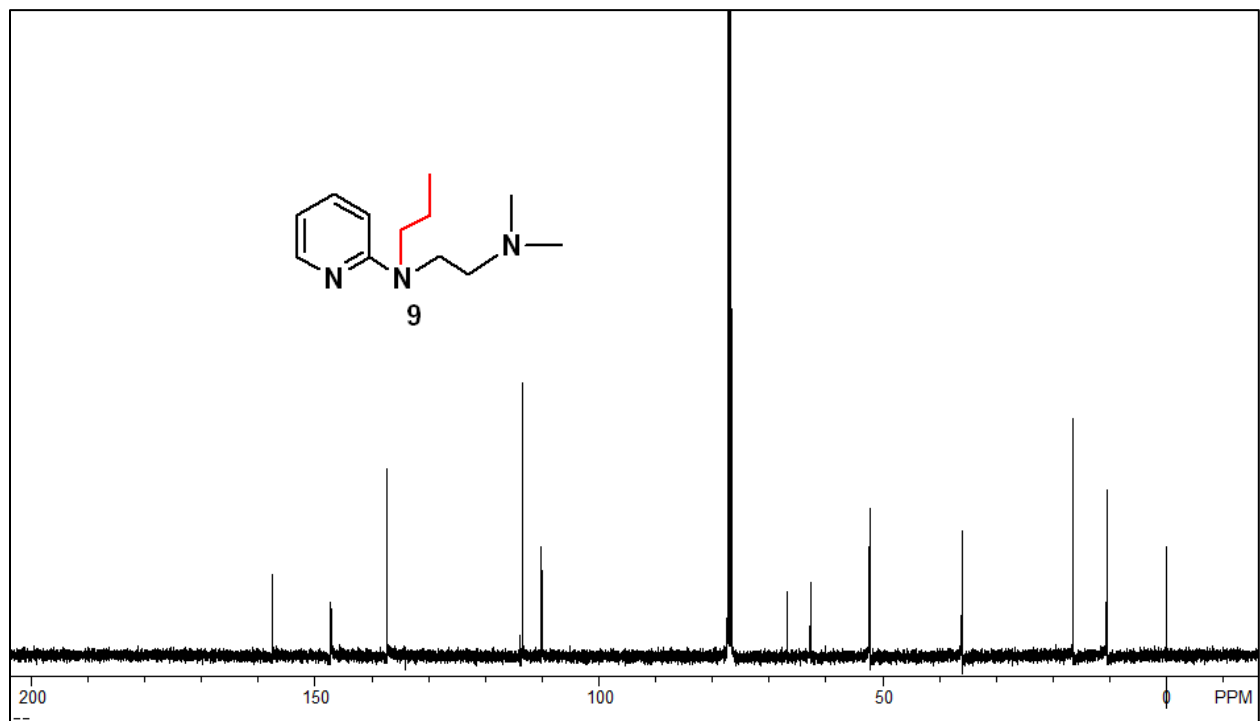
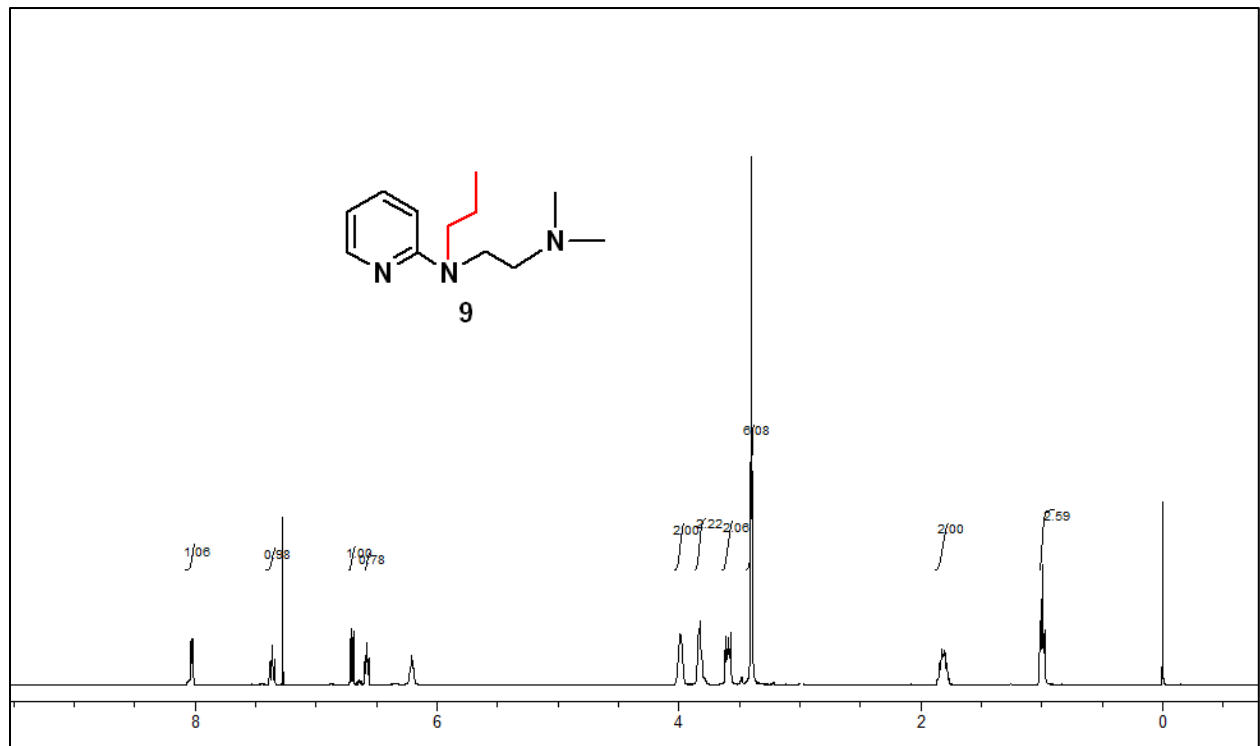


Figure S5

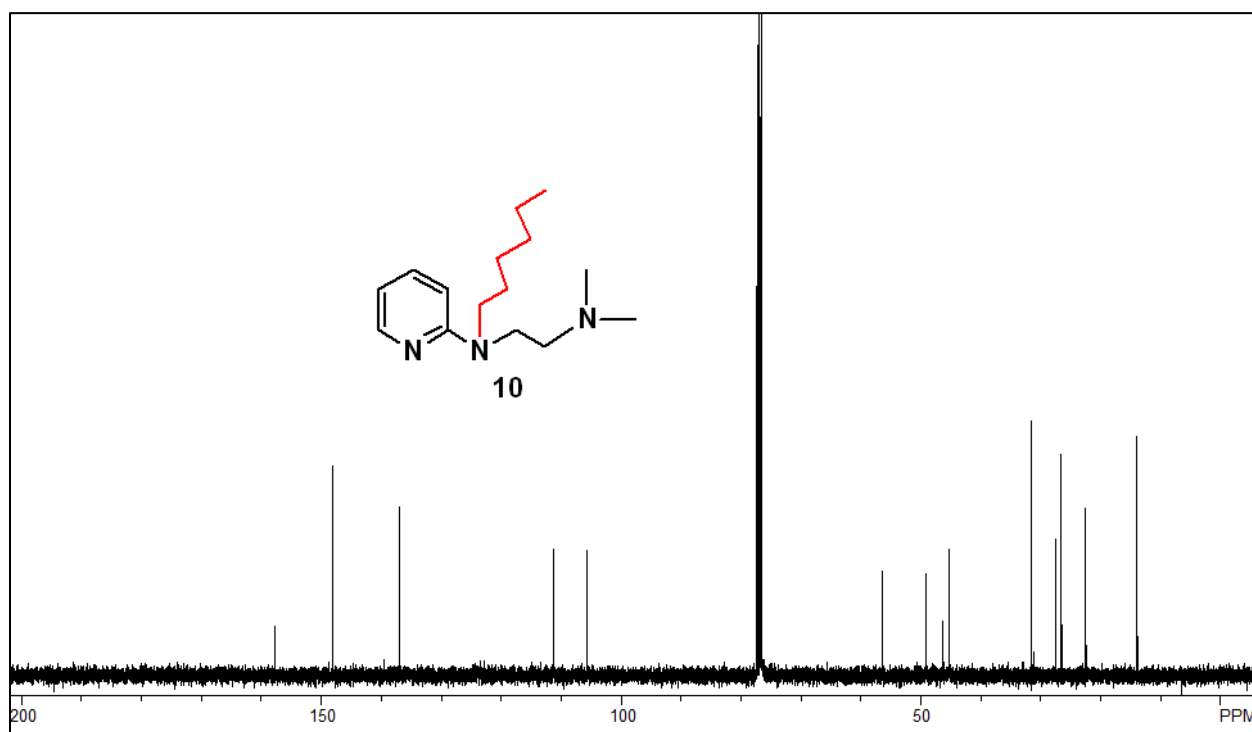
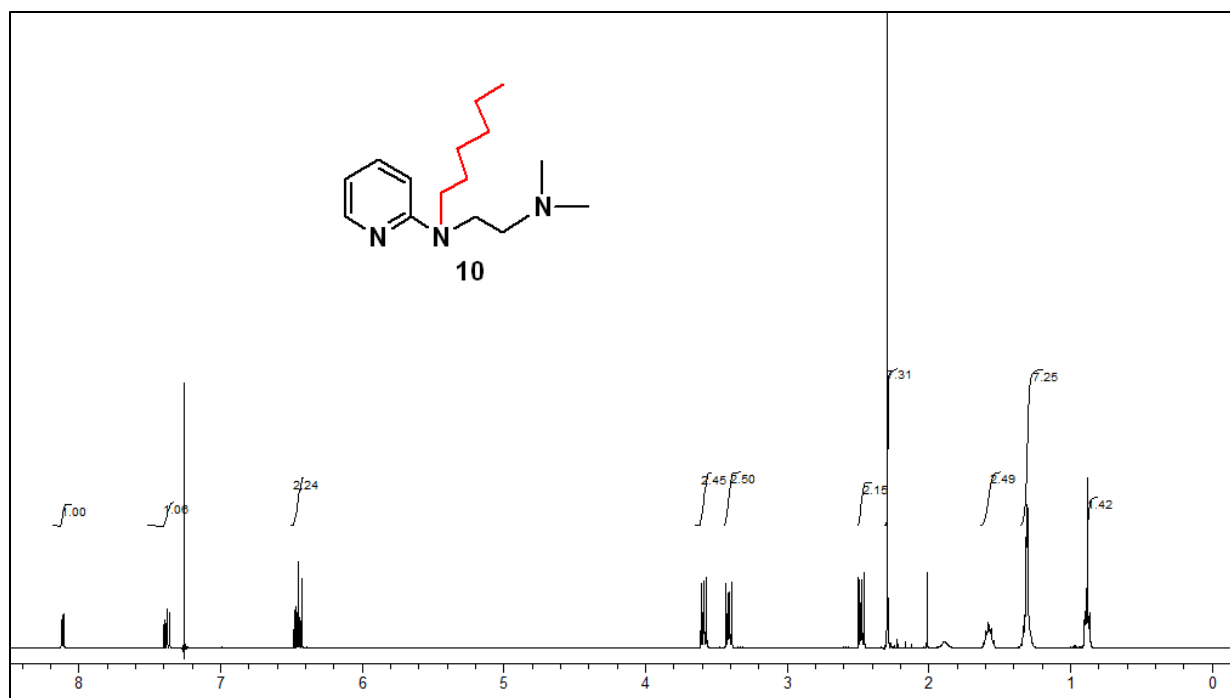


Figure S6

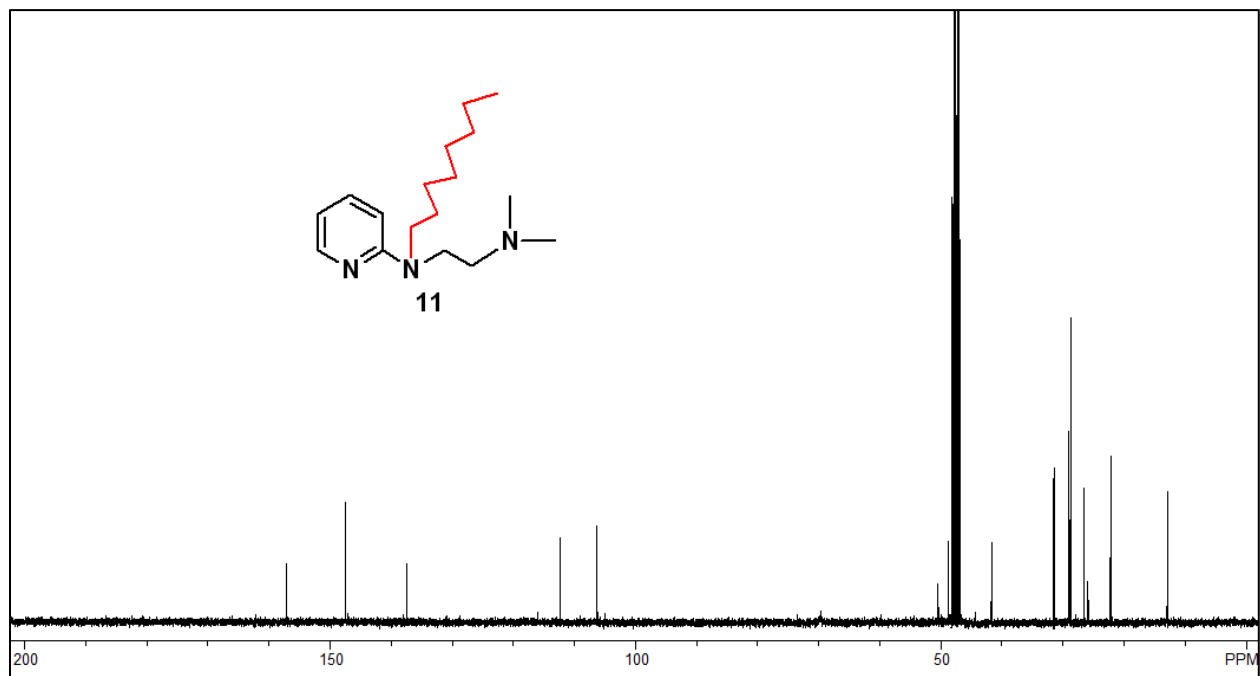
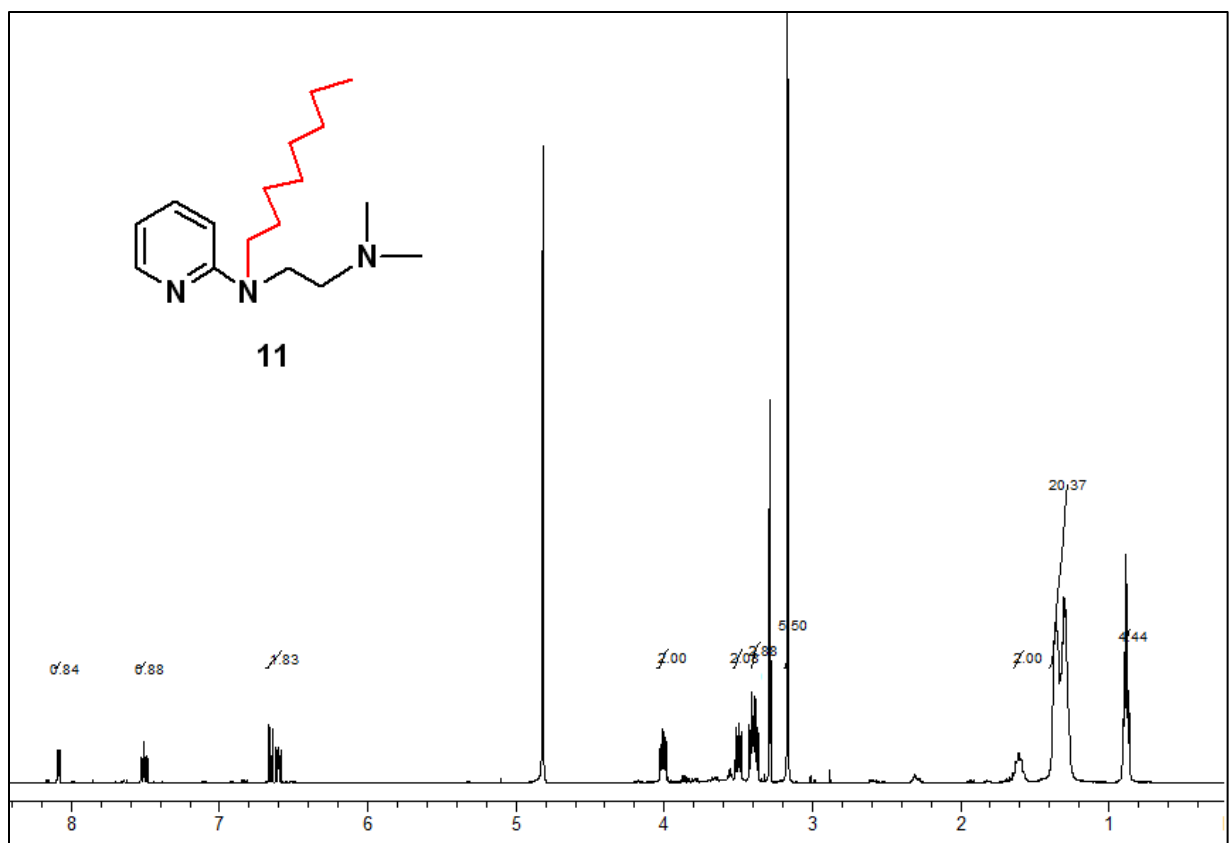


Figure S7



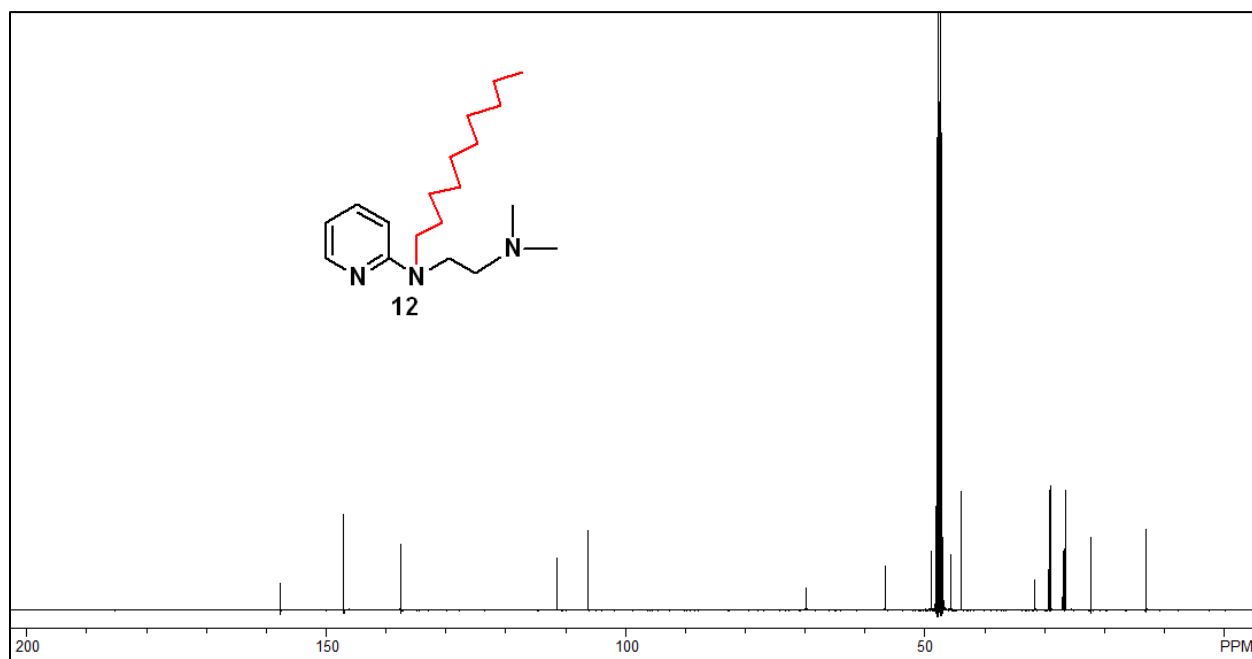
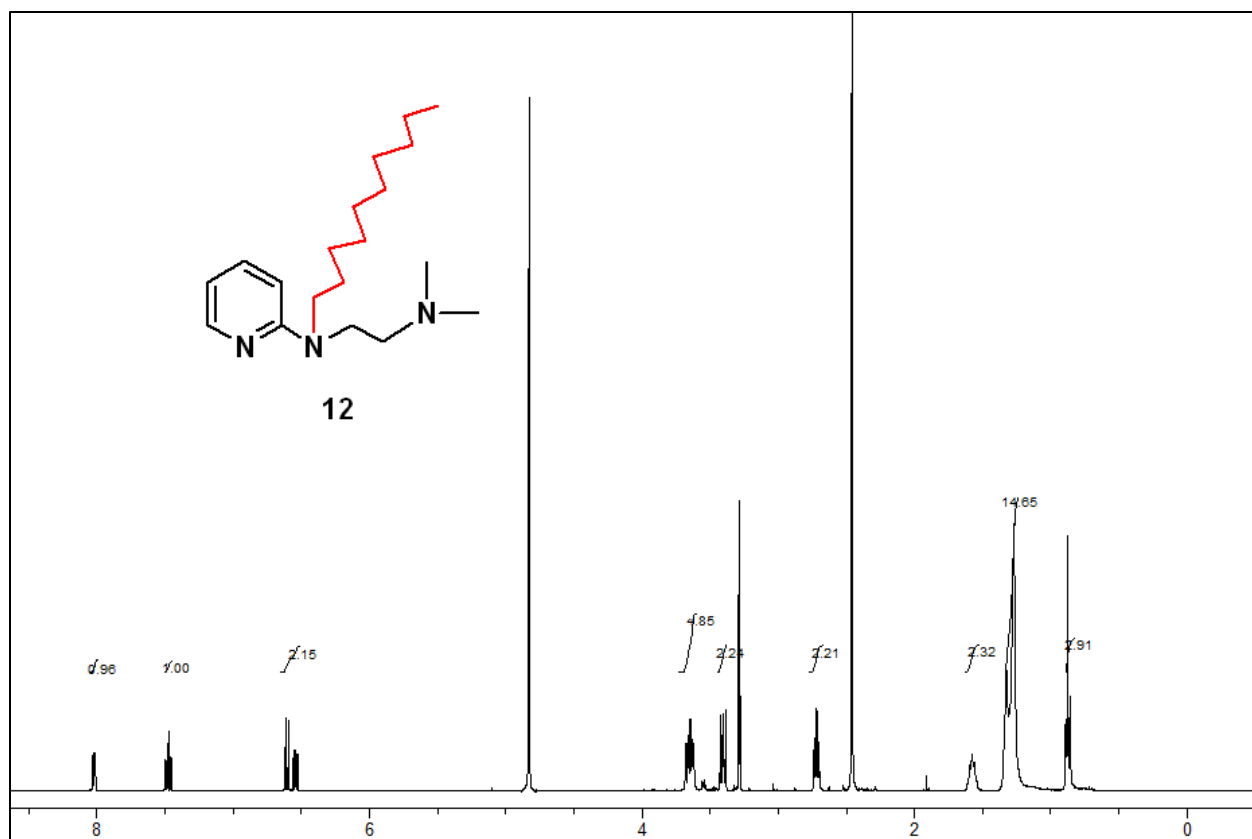


Figure S8

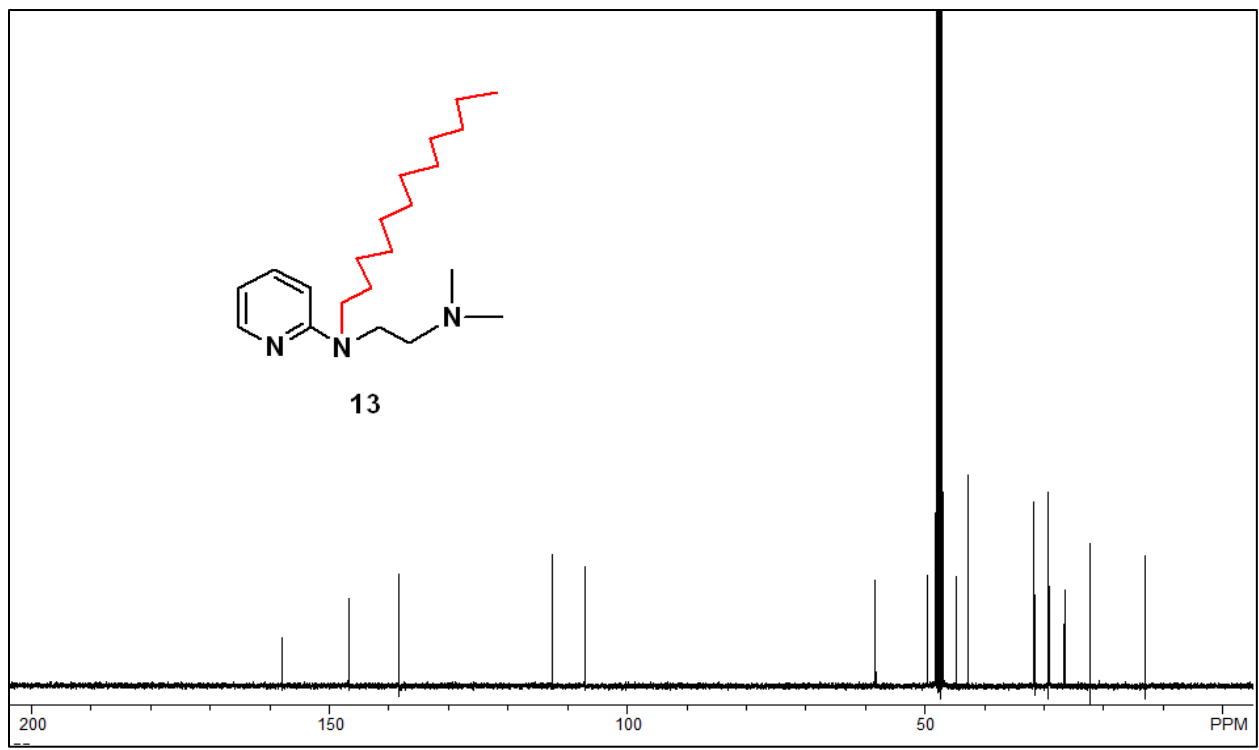
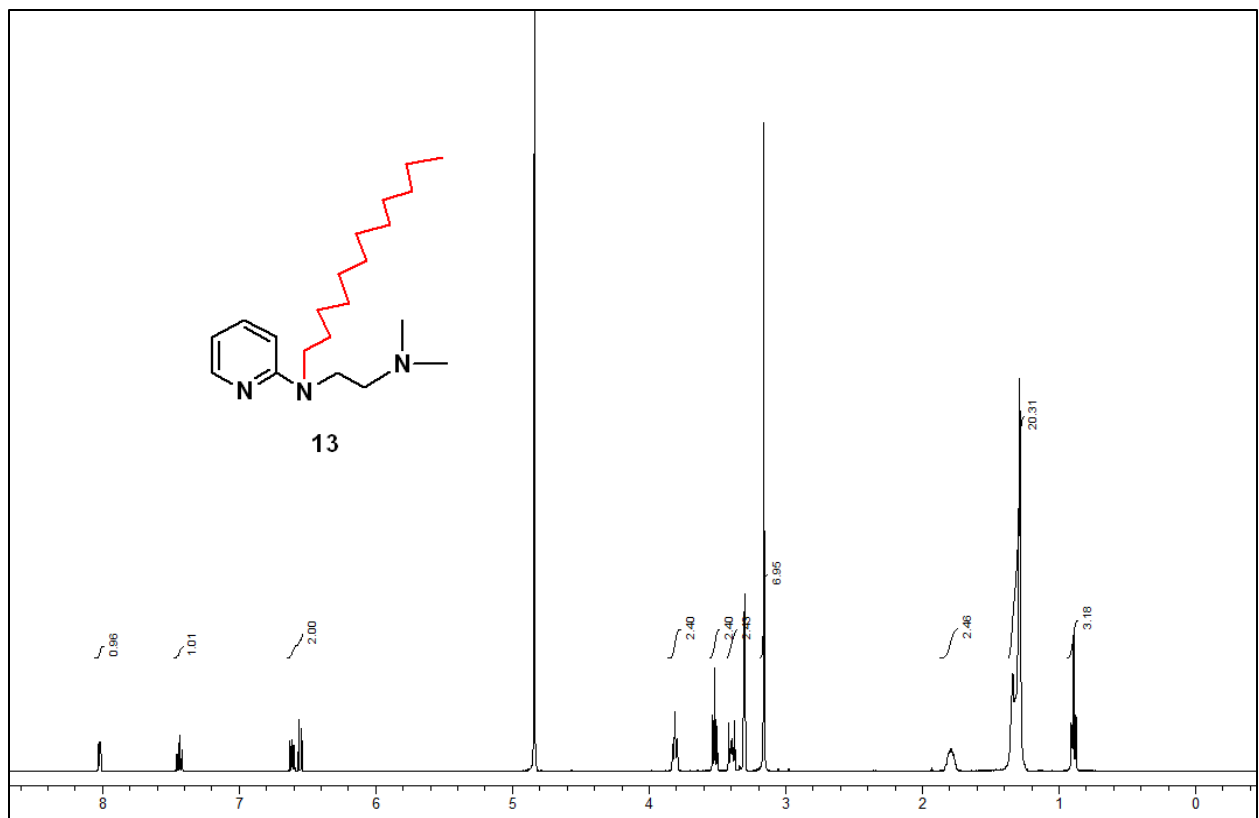


Figure S9

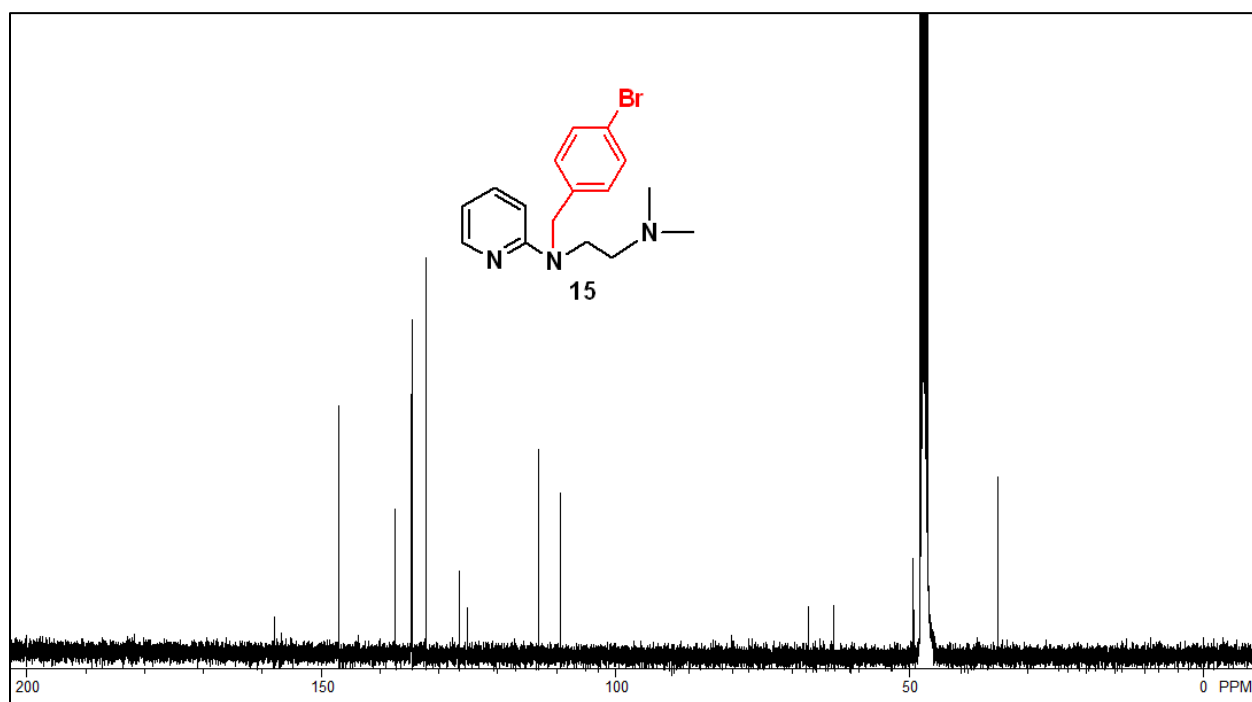
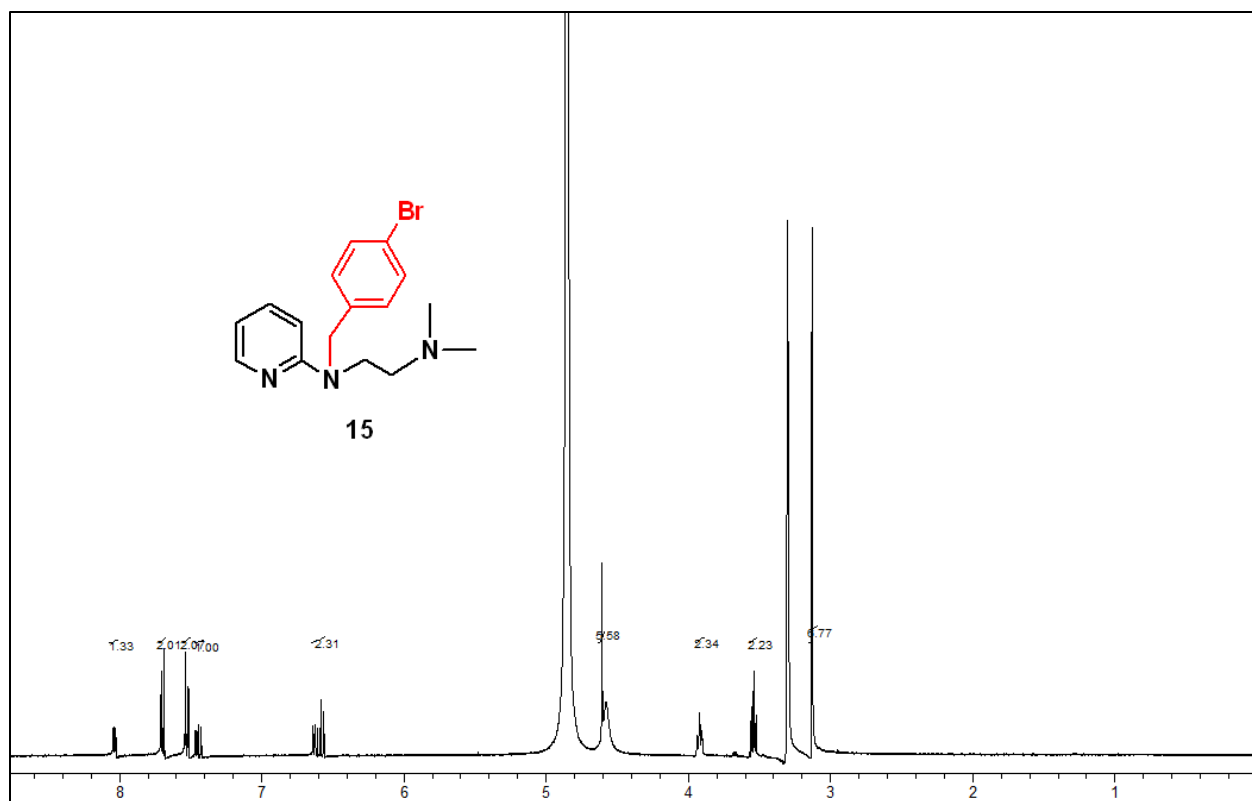


Figure S10

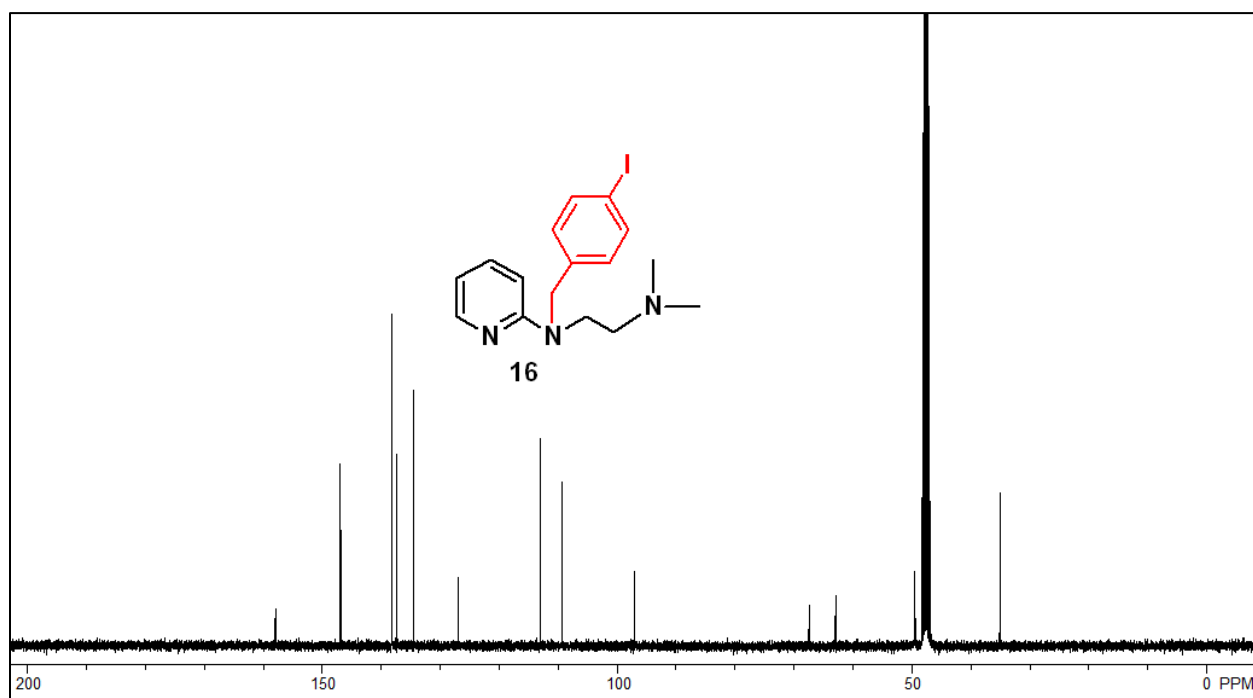
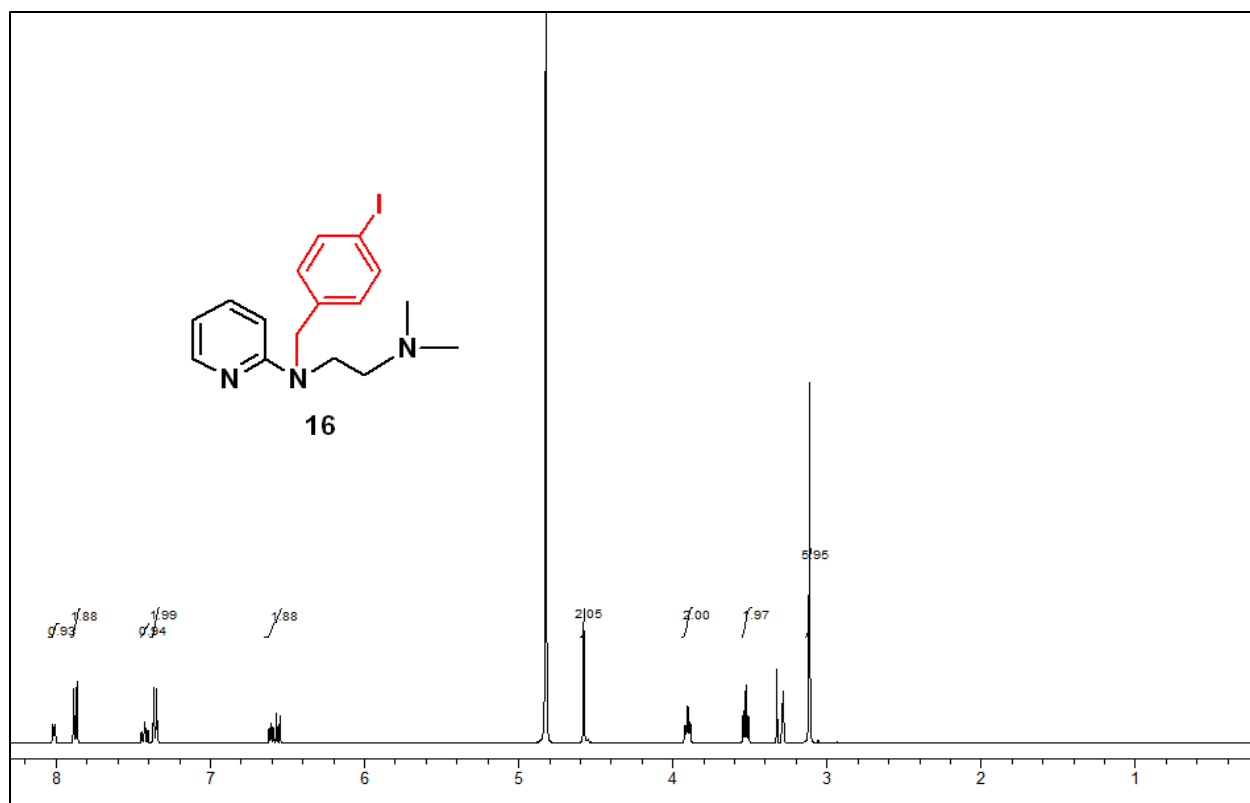


Figure S11

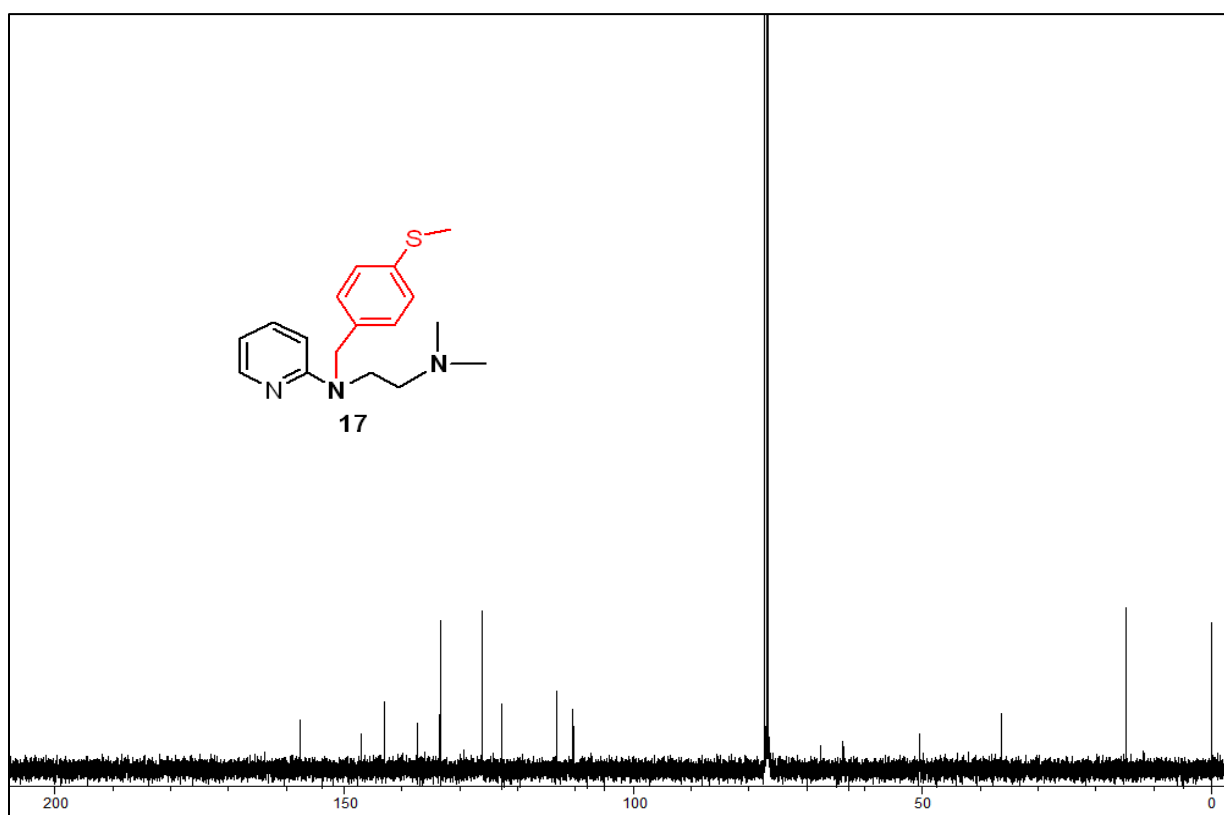
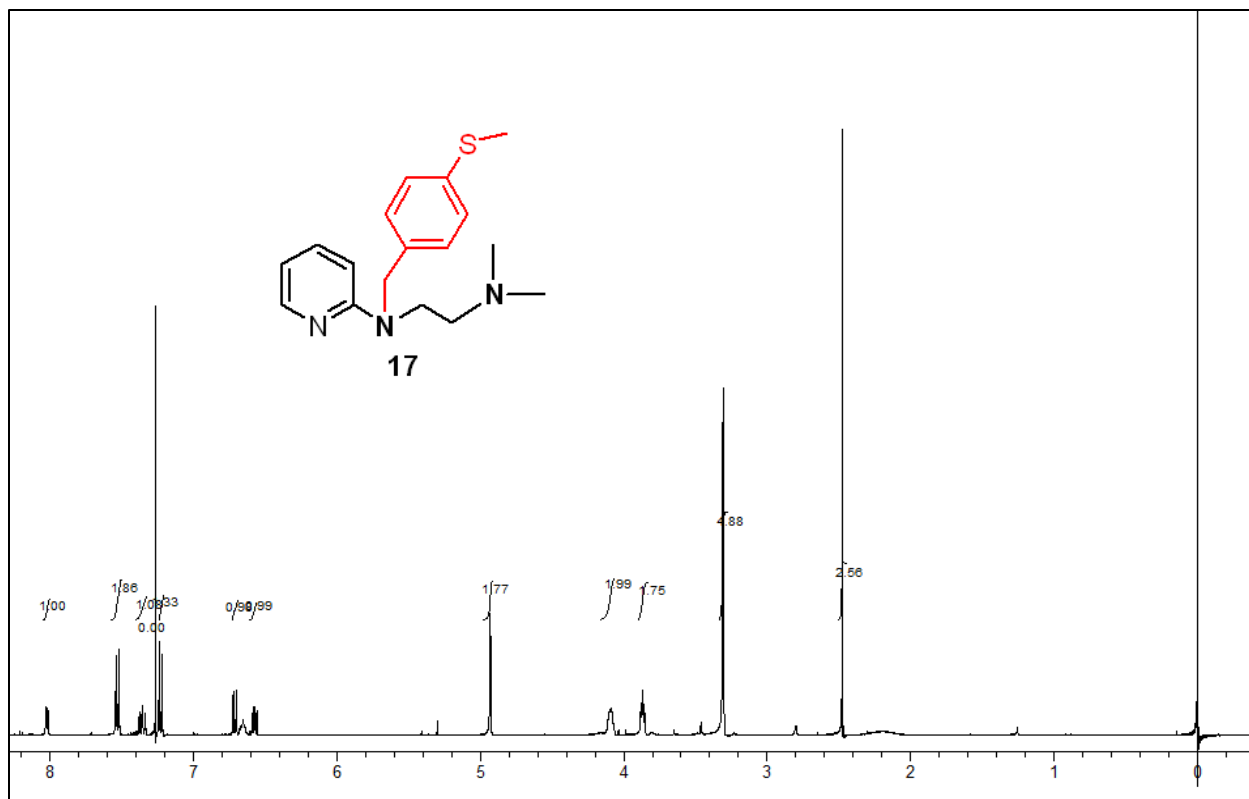


Figure S12

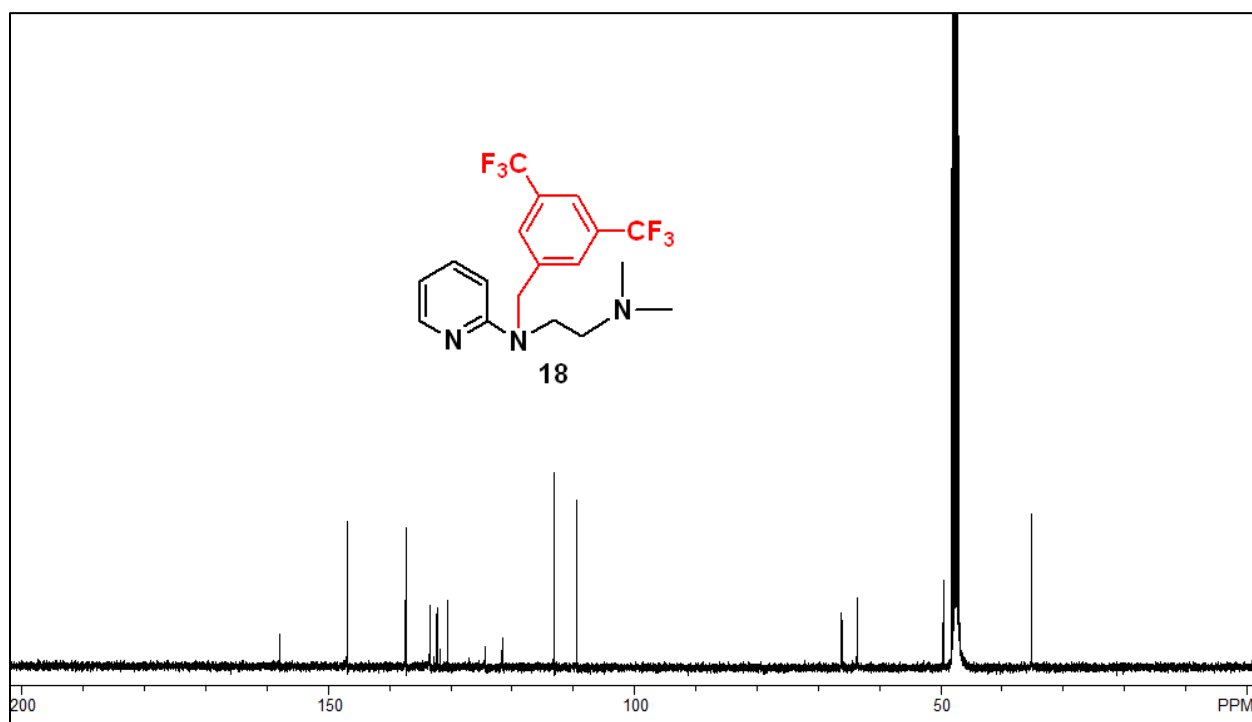
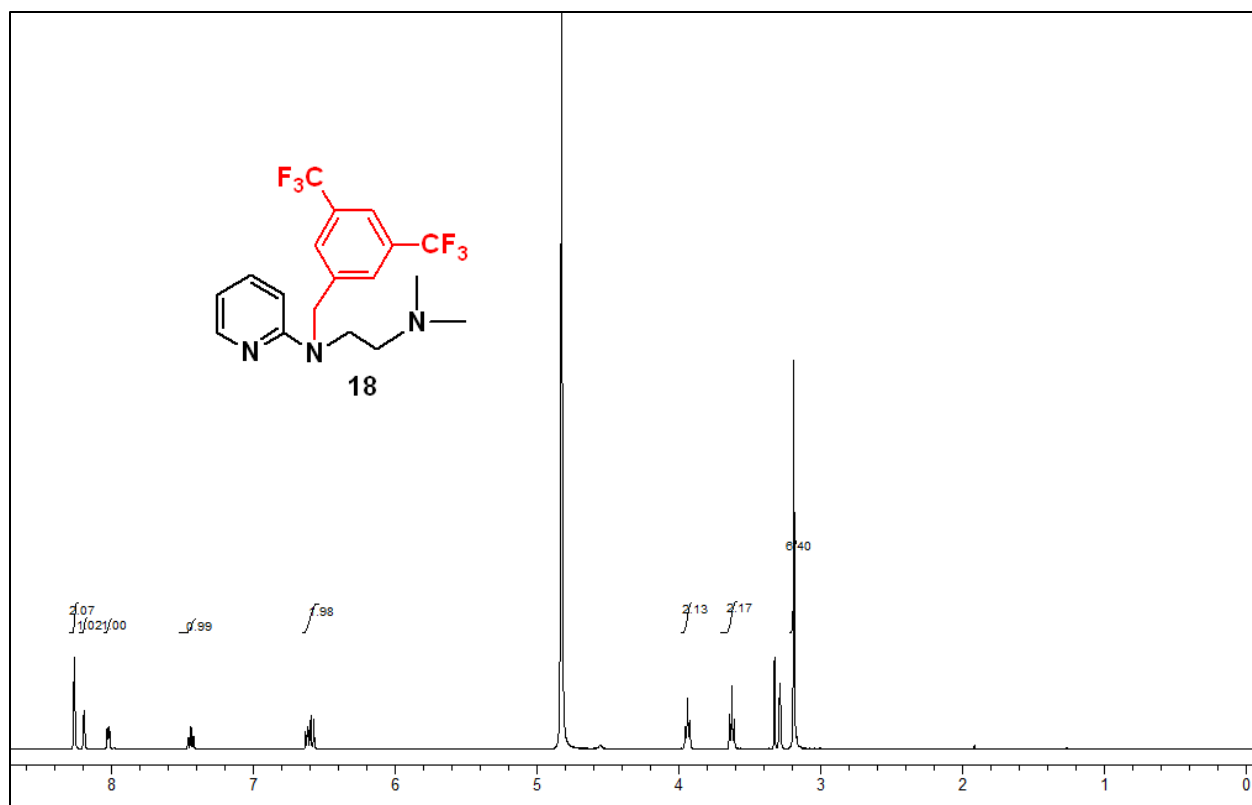


Figure S13

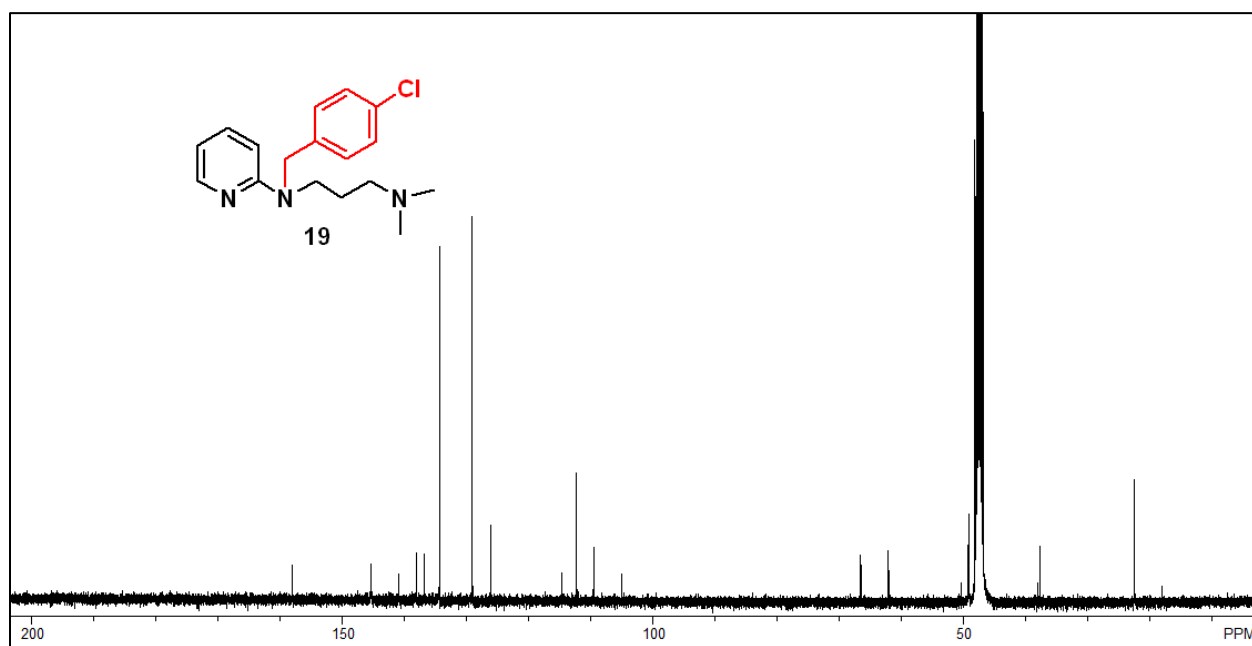
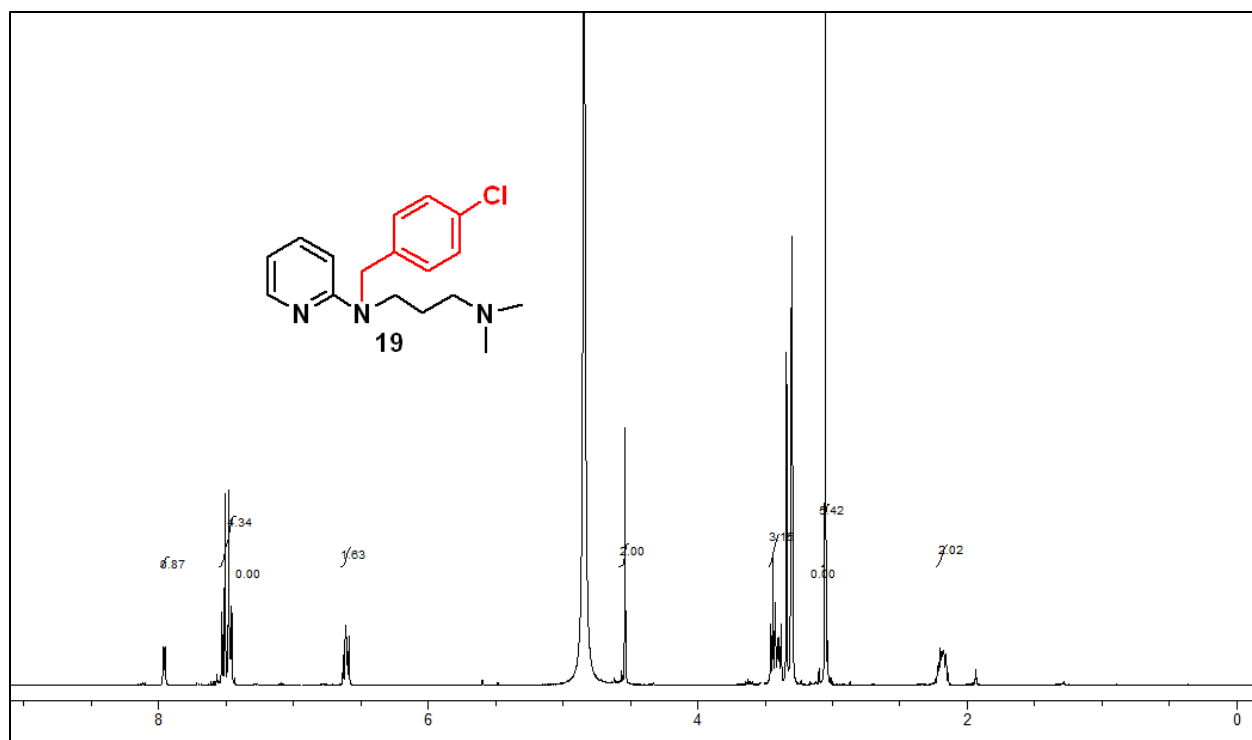


Figure S14

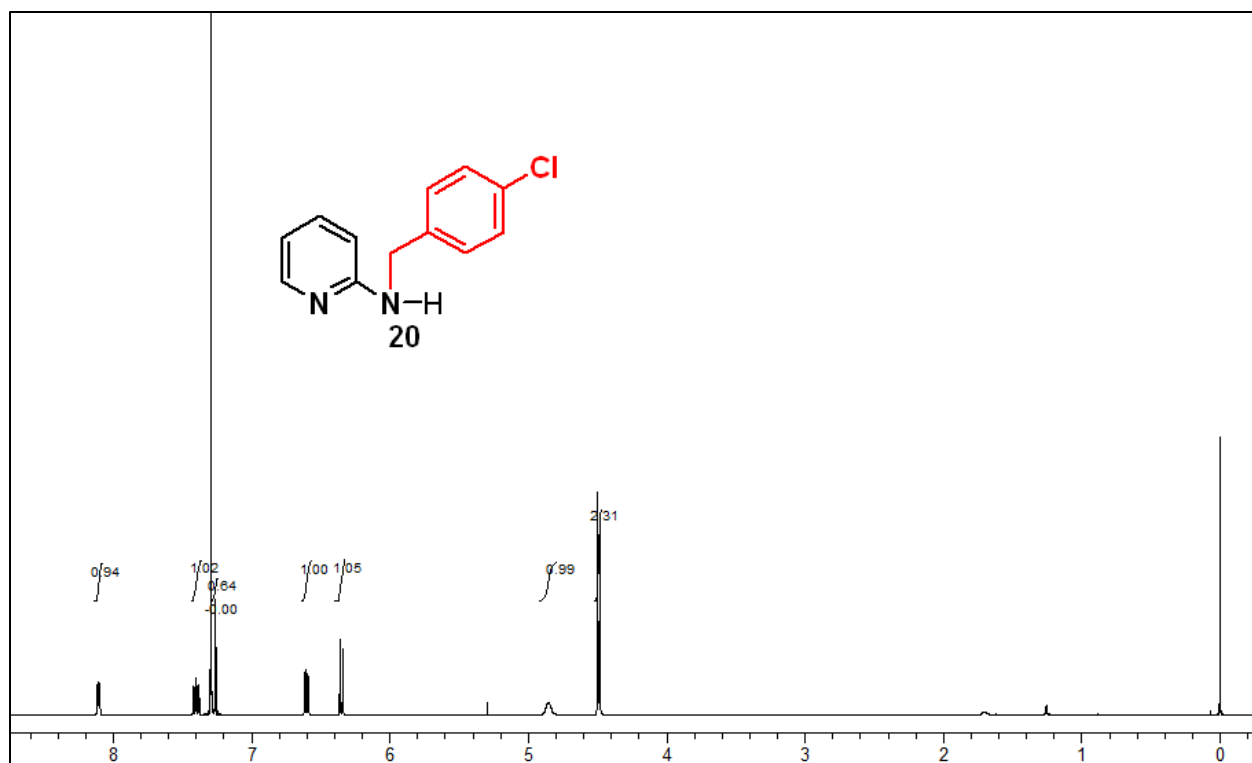


Figure S15



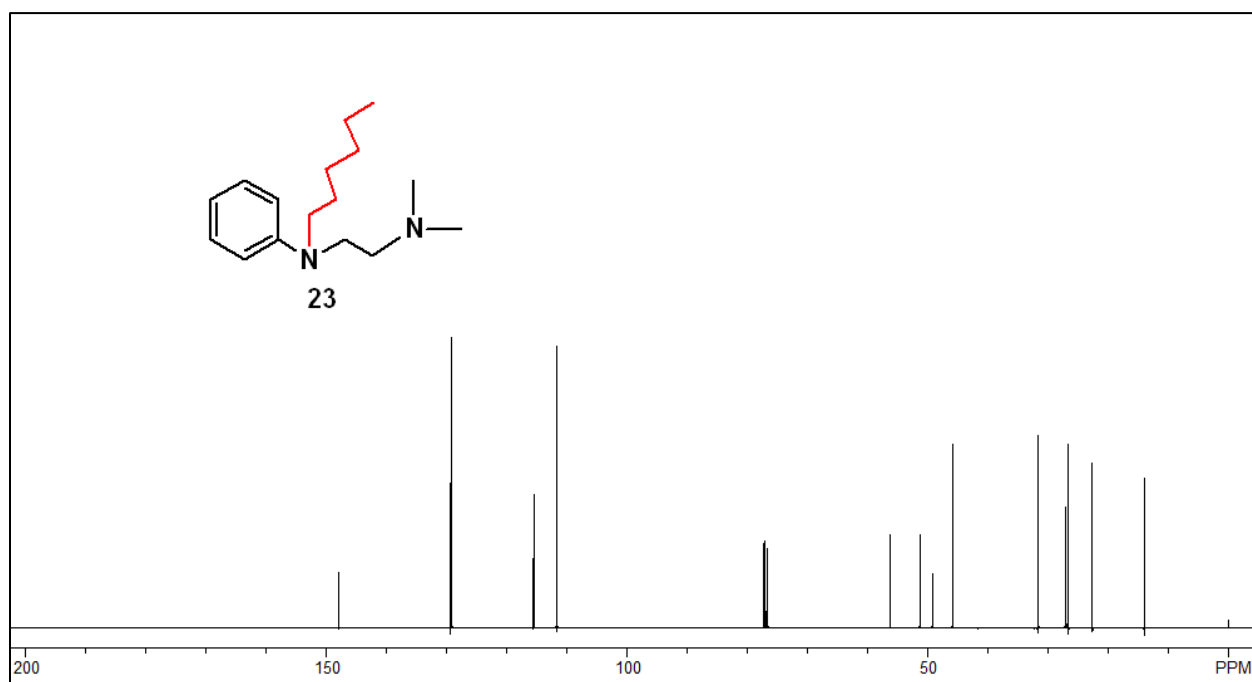
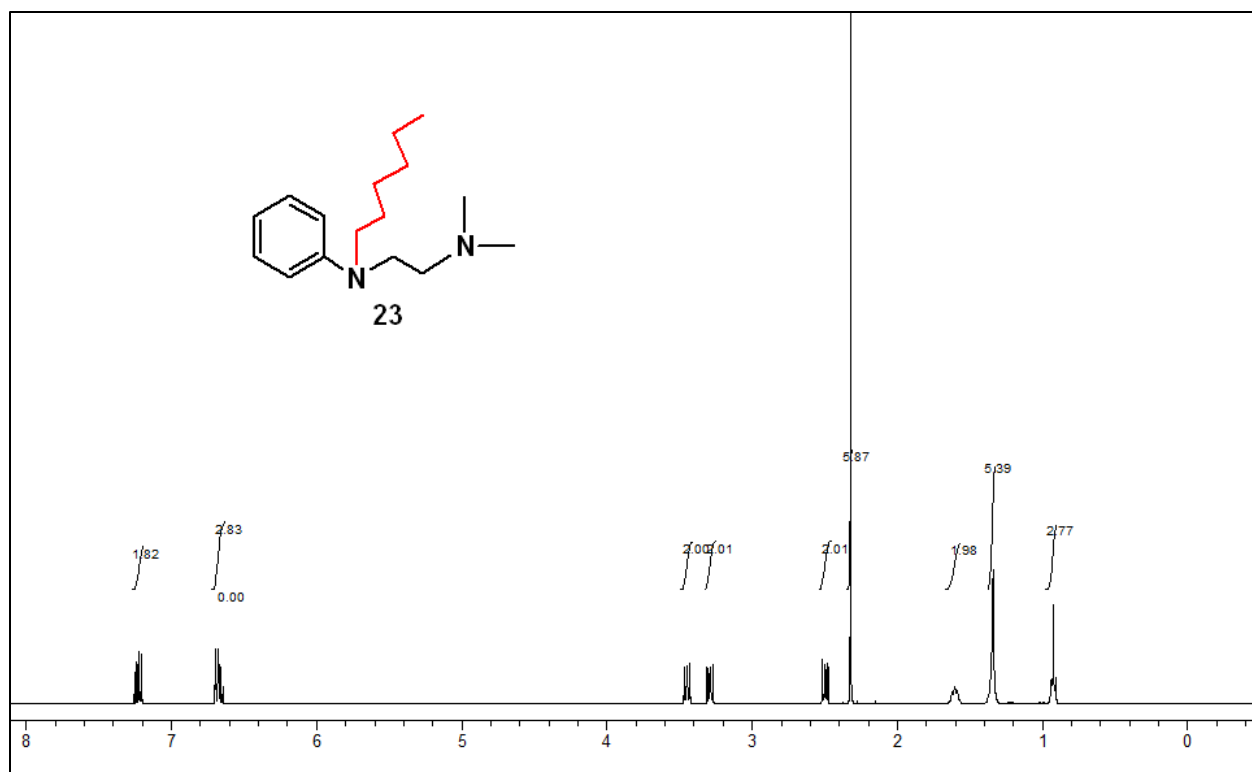


Figure S16

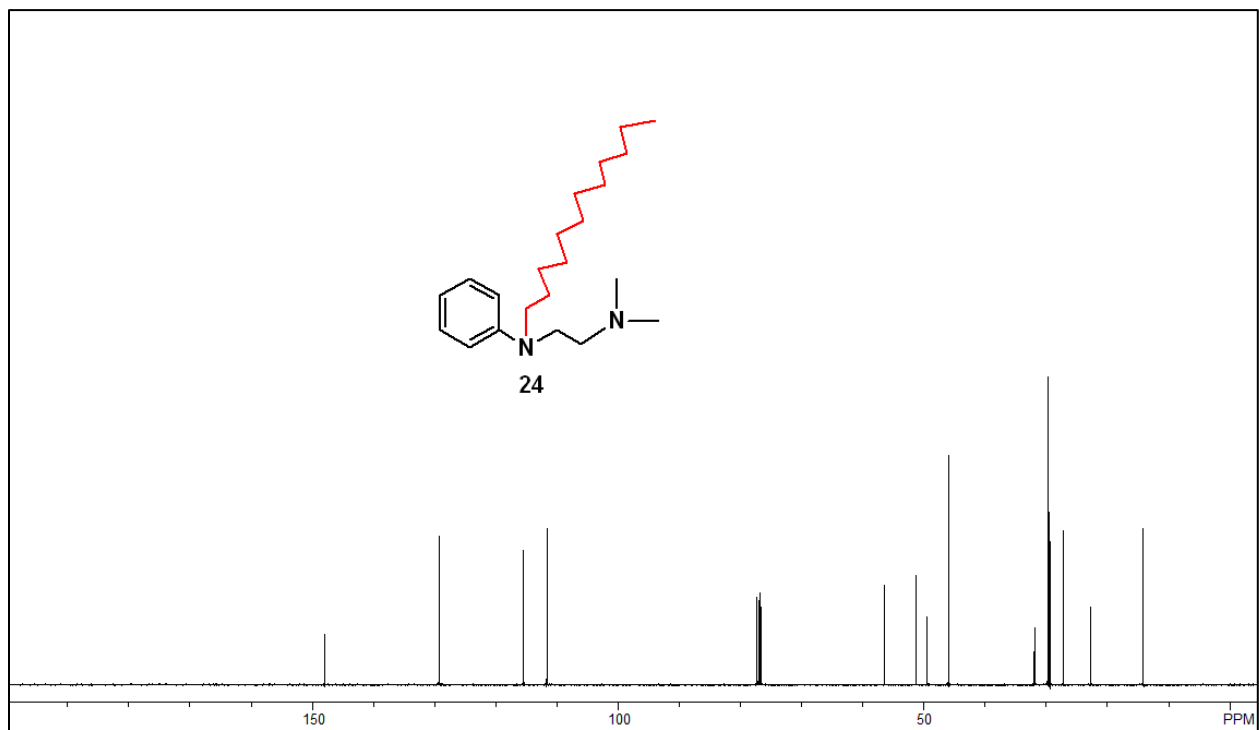
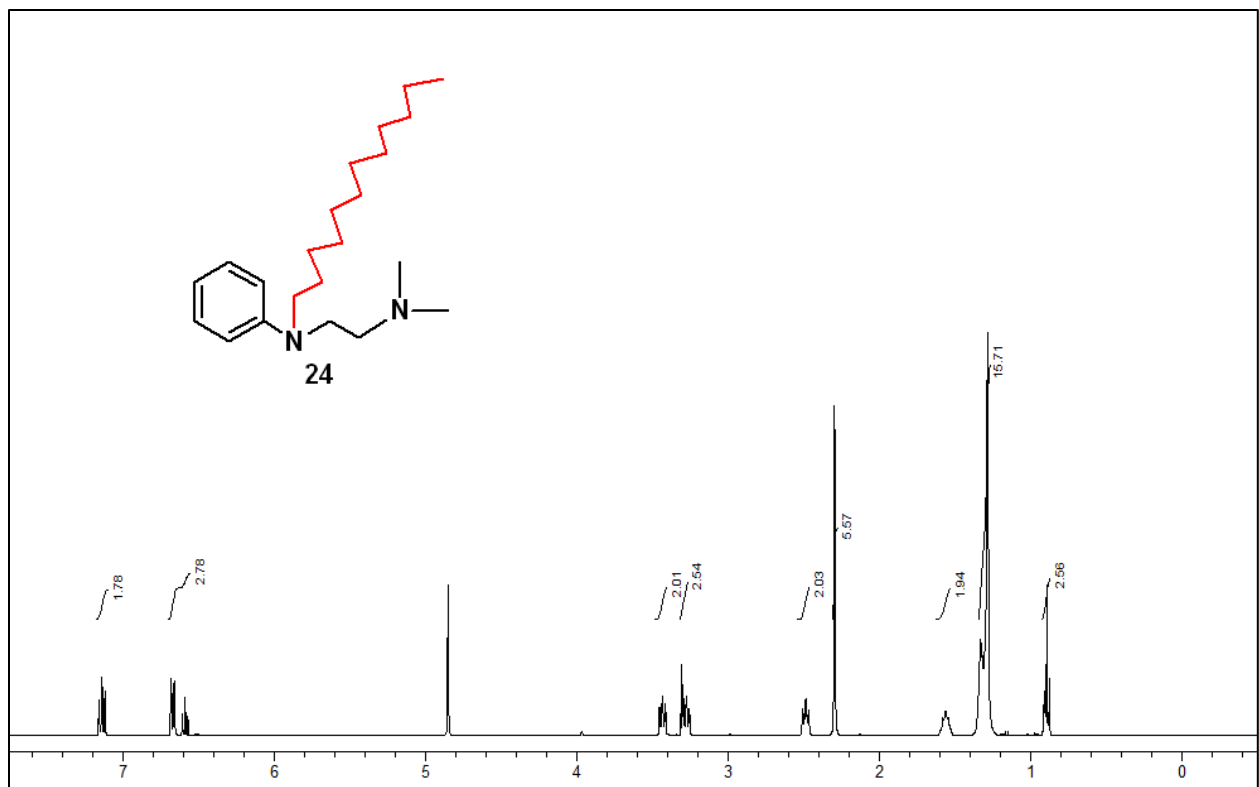


Figure S17

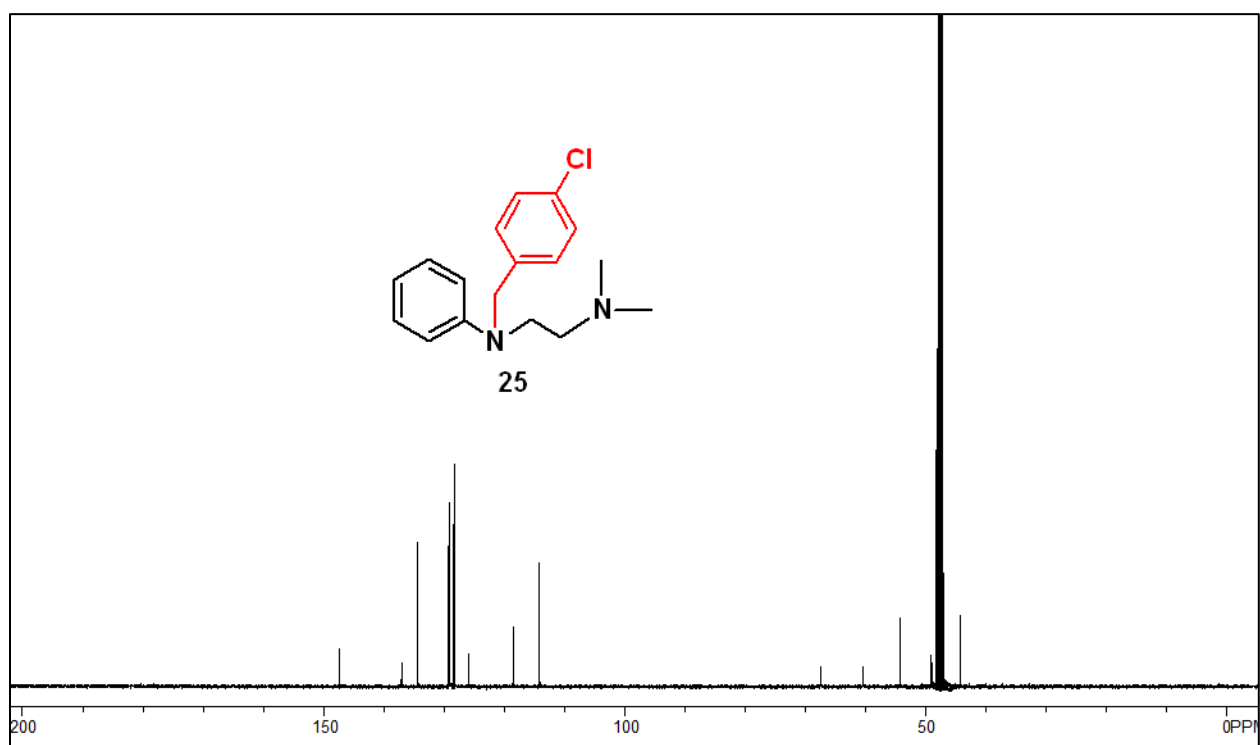
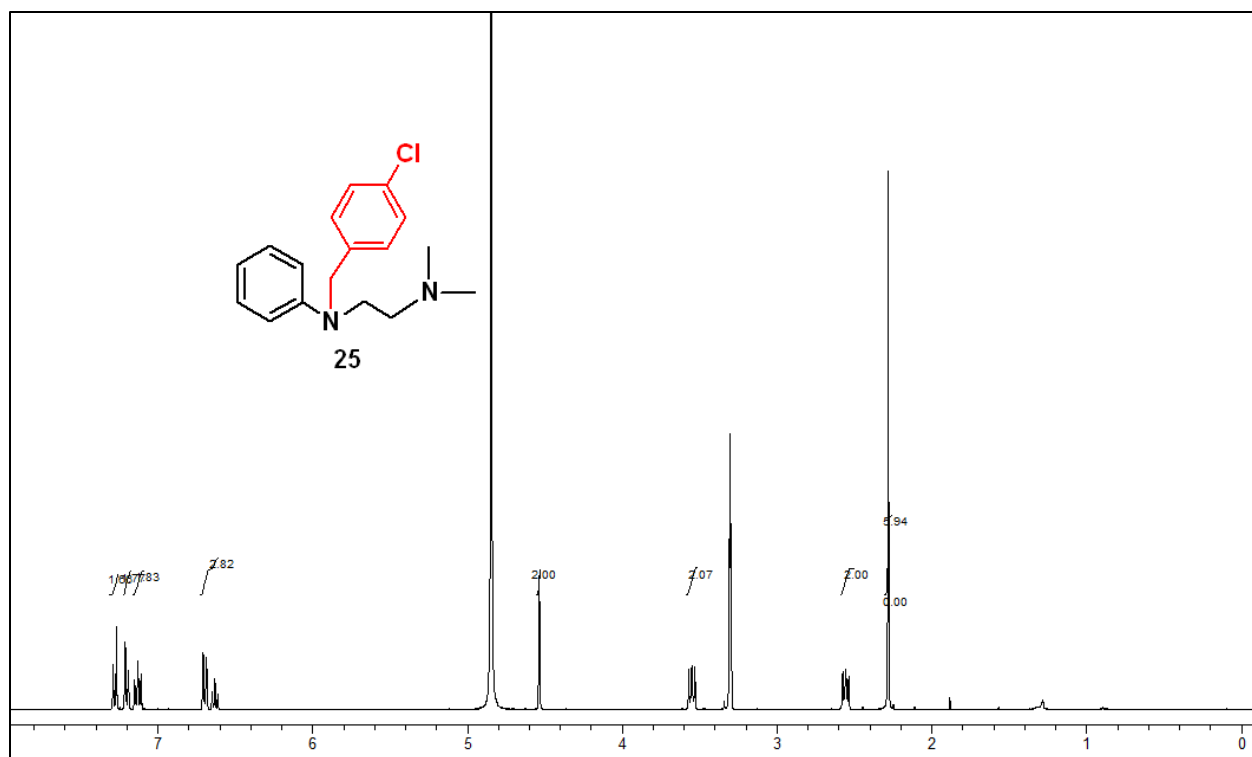


Figure S18

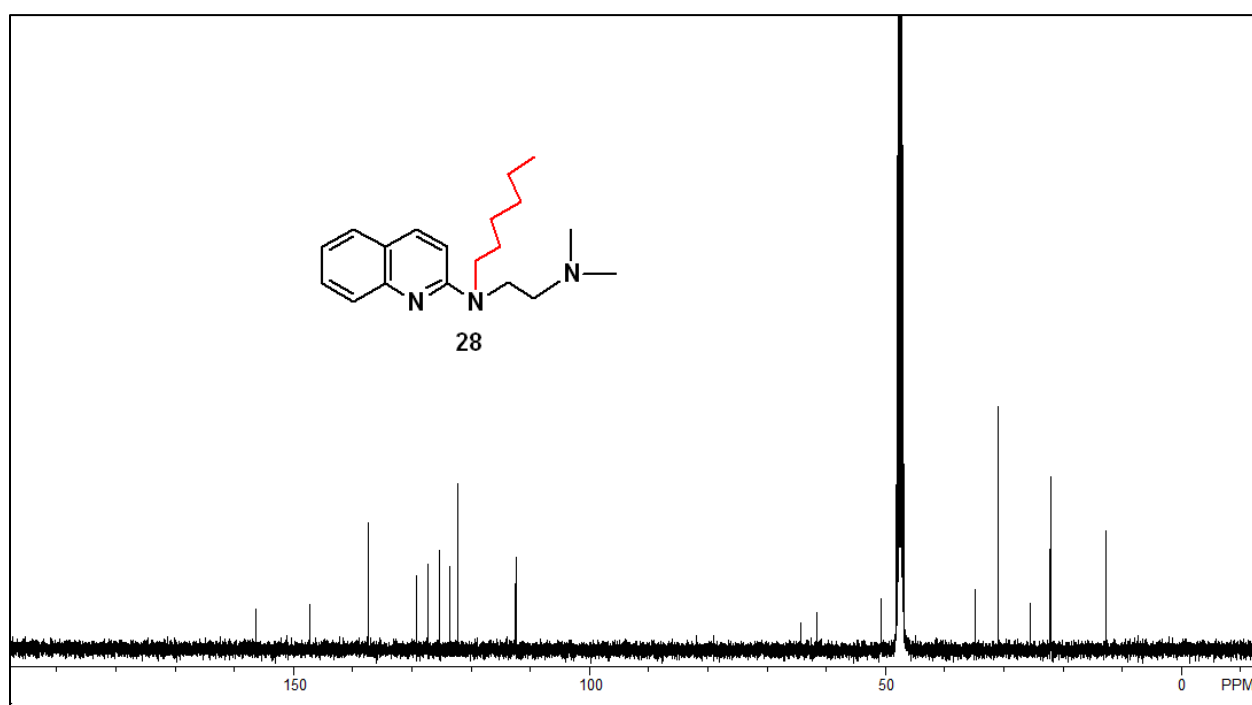
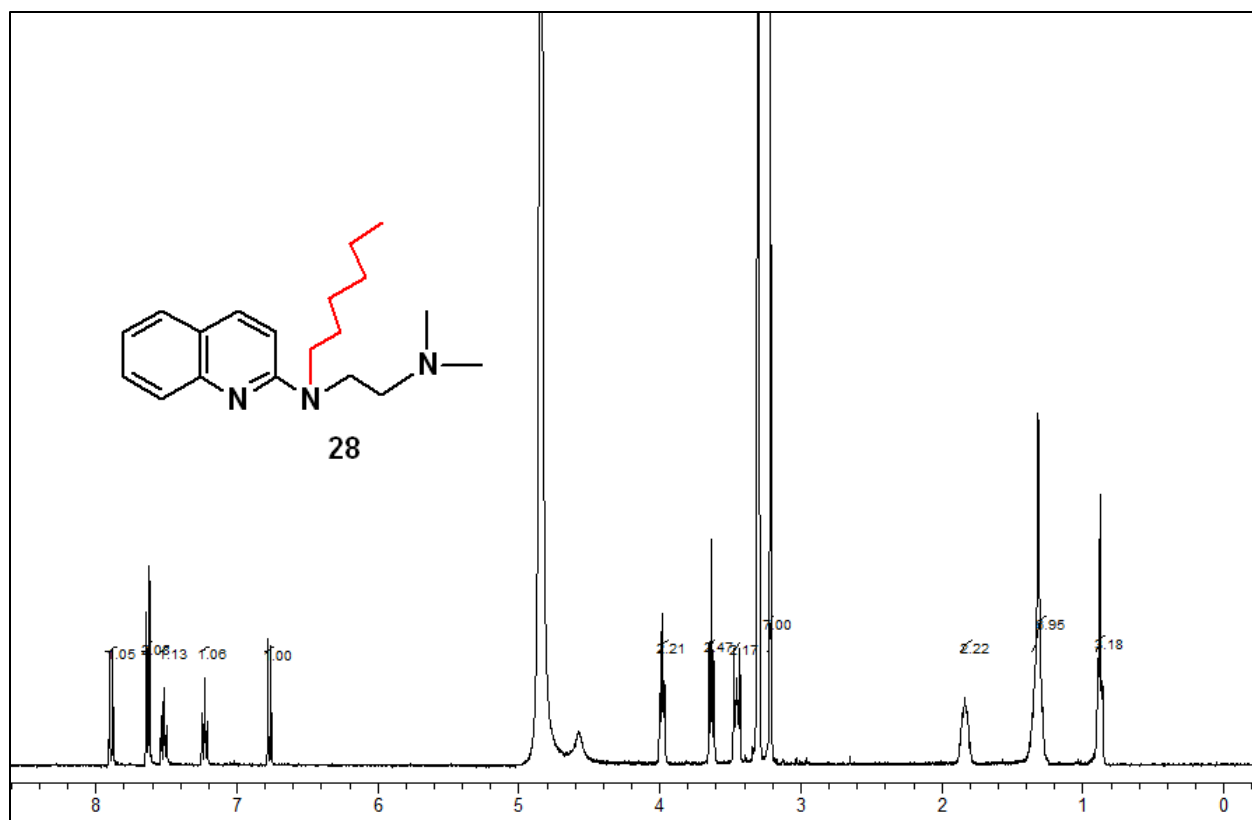


Figure S19

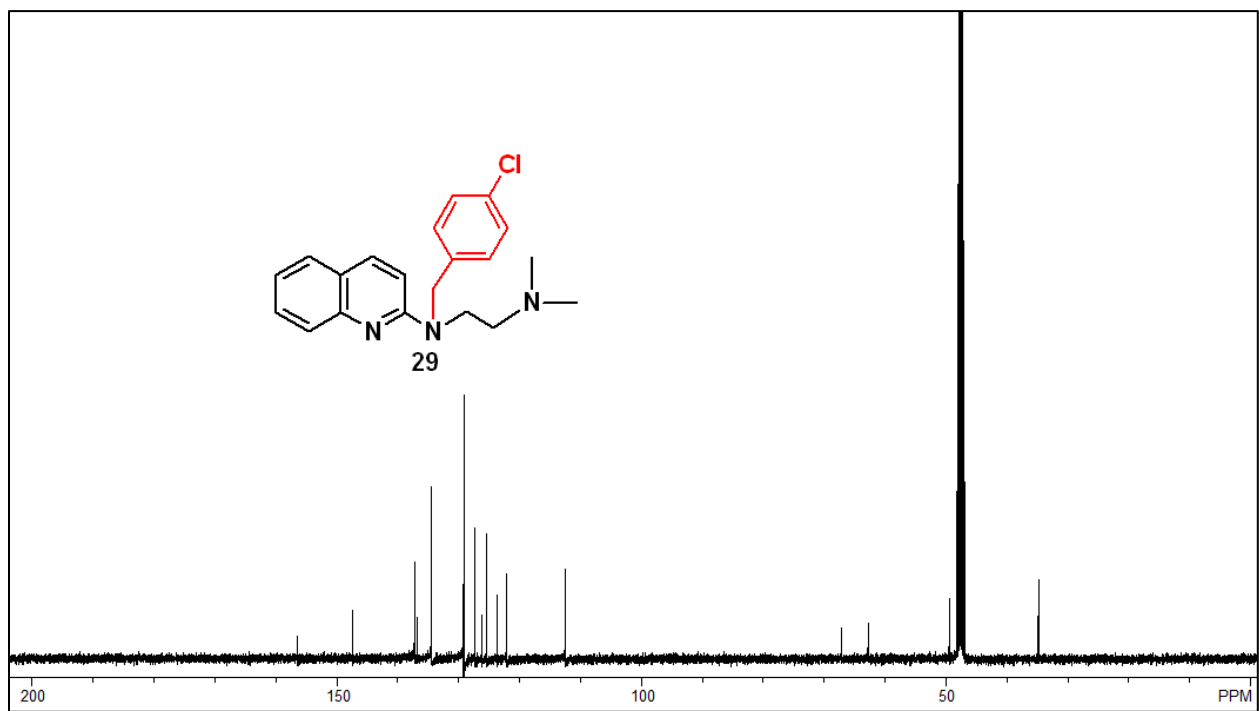
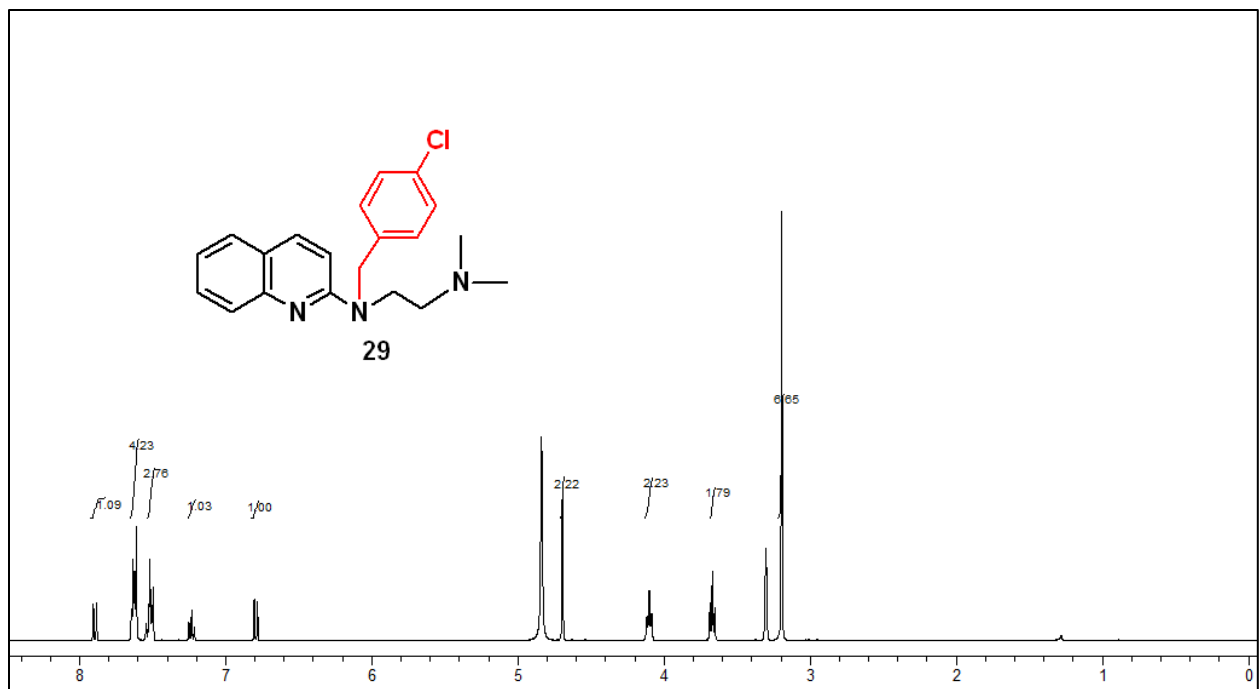


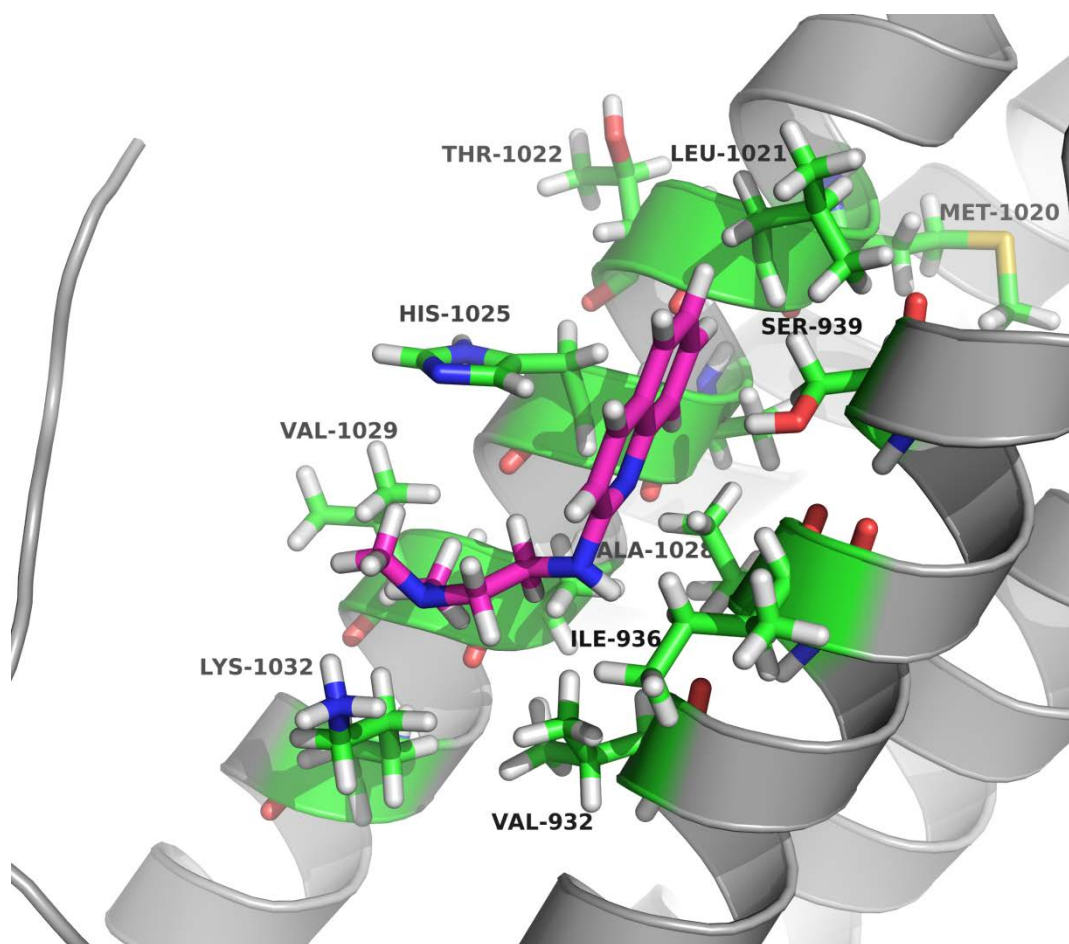
Figure S20

**Table S1.** Log P values of **1** analogs

<b>Compound No.</b>	<b>Log P</b>
1	1.721
7	-1.634
8	-2.053
9	0.364
10	1.295
11	1.962
12	2.723
13	3.712
15	1.771
16	2.030
17	1.792
18	2.847
19	1.650
20	3.086
23	1.563
24	4.883
25	2.087
27	0.277
28	2.653
29	2.704

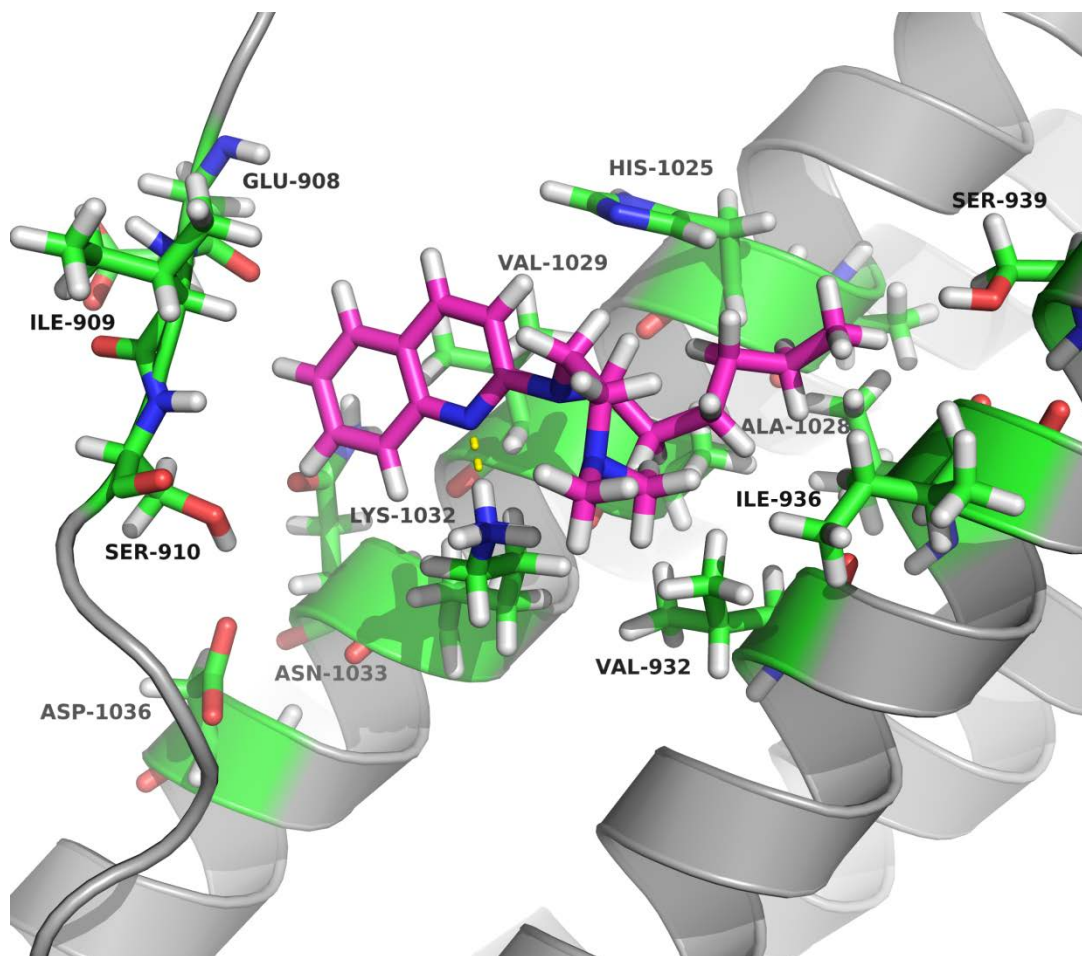
<sup>a</sup>Log P values were calculated using PALLUS software.

**Figure S21.** Predicted binding pose of compound **27** to the FAT domain of FAK.



Ribbon representation of the FAT domain (gray) showing the binding pose of analog **27** (magenta stick) and residues within 5 Angstroms of **27** (green stick).

**Figure S22.** Predicted binding pose of compound **28** to the FAT domain of FAK.



Ribbon representation of the FAT domain (gray) showing the binding pose of analog **28** (magenta stick) and residues within 5 Angstroms of **28** (green stick). A hydrogen bond (yellow dashed line) is formed between the quinoline ring of **28** and Lys 1032.